Nanostructural Complexity

in Polymer Gels and Microgel Packings

Inaugural-Dissertation

to obtain the academic degree

Doctor rerum naturalium (Dr. rer. nat.)

submitted to the Department of Biology, Chemistry and Pharmacy

of Freie Universität Berlin

by

FANY DI LORENZO

from Florence, Italy

2015

This work was carried out from April 2012 until July 2015 under the supervision of Prof. Dr. Sebastian Seiffert at Helmholtz-Zentrum Berlin, in the Institute of Soft Matter and Functional Materials.

1st Reviewer: Prof. Dr. Sebastian Seiffert

2nd Reviewer: Prof. Dr. Matthias Ballauff

Date of defense: 27.10.2015.

Acknowledgments

First of all, I would like to thank Prof. Sebastian Seiffert for his supervision and for his scientific and personal support all over the course of my doctoral studies. Under his guidance I had the opportunity to work on many interesting and challenging research projects.

Moreover, Prof. Matthias Ballauff is gratefully acknowledged for co-reviewing this thesis and for having hosted me in special research labs at Helmholtz-Zentrum Berlin.

I very much enjoyed working with the members of the fast-growing Seiffert group, as well as with all members of the Ballauff group. In particular, I would like to thank Dr. Miriam Siebenbürger for assistance with the rheometers, and Dr. Torsten Rossow for having introduced me both to confocal fluorescence microscopy and to soft lithography.

My collaboration partners, Johannes Hellwig and Prof. Regine von Klitzing from the Technical University Berlin, along with Miroslava Racheva and Dr. Christian Wischke from Helmholtz-Zentrum Geesthacht, are gratefully acknowledged for stimulating discussions and fruitful cooperation. I also thank Marlies Gräwert from the Max Planck Institute of Colloids and Interfaces for performing SEC analyses.

The following bachelor and master students of the Free University Berlin carried out research internships under my co-supervision, and are kindly acknowledged: Enrico Miceli, Michael Giulbudagian, Emanuel Glitscher, Viviane Wagner and Gülsah Ayvalik.

The Helmholtz Virtual Institute “Multifunctional Biomaterials for Medicine” is acknowledged for funding.

A special thanks goes to Dr. Torsten Rossow for having read parts of this manuscript, as well as to Dr. Miriam Siebenbürger, Matthew Barrett and Christian Balz for linguistic reviewing.

Finally, I would like to thank my family for their constant support throughout my education.

Contents

List of Symbols (Latin Letters)

c	Concentration of a microgel suspension or of a polymer solution
C_m	Concentration of a particle suspension corresponding to φ=0.64
c_P	Polymer concentration within a microgel particle
d	Number density of particles per unit volume
D	Diffusion coefficient
f	Crosslink functionality
F	Friction coefficient
G'	Elastic or storage modulus
G''	Viscous or loss modulus
G_P'	Plateau storage modulus
k_B	Boltzmann constant
M_w	Molecular weight
n	Stiffness of the repulsive pair potential
N	Number of beads in a polymer chain
Pe	Péclet number
q	Scattering vector
r	Interparticle distance
R	Particle radius
R_{ex}	Excess scattering intensity
t	Time
T	Temperature
U	Repulsive pair potential
V_d	Volume of a swollen particle in the dilute limit

List of Symbols (Greek Letters)

γ	Strain
ε	Elastic energy
ζ	Packing fraction
η	Viscosity
θ	Scattering angle

λ	Wavelength of incident radiation
μ	Refractive index
ν	Concentration of elastic chains in a polymer network
ν_{eff}	Concentration of effective elastic chains in a polymer network
ξ	Mesh size
Ξ	Correlation length of static inhomogeneities
σ	Sum of the radii of two particles
τ	Shear stress
τ_{α}	Alpha relaxation time
τ_{β}	Beta relaxation time
τ_{B}	Brownian time
τ_{C}	Characteristic time
τ_{Rep}	Reptation time
φ	Volume fraction
φ_{cp}	Volume fraction of hexagonal close packing
φ_{freeze}	Volume fraction of the freezing point
φ_{g}	Volume fraction of the glass transition
φ_{rcp}	Volume fraction of random close packing
ω	Angular oscillation frequency

List of Abbrevations

AAm	Acrylamide
AFM	Atomic force microscopy
APS	Ammonium persulfate
BIS	*N*,*N*′-methylenebis(acrylamide)
DLS	Dynamic light scattering
DMMI	Dimethylmaleimide
DMMIAAm	(Dimethlymaleimide)ethylacrylamide
FRAP	Fluorescence recovery after photobleaching
HS	Hard sphere
LCST	Lower critical solution temperature

MASI	*N*-(methacryloxy)succinimide
MCT	Mode couple theory
NMR	Nuclear magnetic resonance
NASI	*N*-acryloxysuccinimide
NIPAm	*N*-isopropylacrylamide
PAAm	Poly(acrylamide)
PDMS	Poly(dimethylsiloxane)
PMMA	Poly(methyl methacrylate)
PNIPAm	Poly(*N*-isopropylacrylamide)
PS	Polystyrene
SANS	Small angle x-ray scattering
SAXS	Small angle neutron scattering
SDS	Sodium dodecyl sulfate
SSP	Soft-sphere potential
TEMED	Tetramethylethylenediamine
TXS	Thioxanthone-disulfonate
UCST	Upper critical solution temperature
UV	Ultraviolet light

1 Introduction

1.1 Polymer Gels

1.1.1 Definition and Applications of Polymer Gels

Polymer gels consist of polymer networks swollen in a solvent.[1,2] Polymer networks are three-dimensional assemblies of covalently or physically crosslinked macromolecular chains.[3]

If polymer networks are swollen in water, they are called *hydrogels*; if, in contrast, they are swollen in an organic solvent, they are denoted as *organogels*. Polymer gels can also be classified according to their size: gels exhibiting sizes that range from a few nanometers to several hundreds of micrometers are commonly referred to as *microgels*,[4] whereas gels of larger size are called *macrogels* or simply *gels,* as shown in Figure 1.1. Synthetic hydrogels find an increasing amount of applications in absorbent[5] and separation[6–10] technology, controlled drug delivery,[11–16] catalysis,[17–19] and in the mimic of biological tissues.[20] Examples of synthetic hydrogels commonly used in everyday life are sodium polyacrylate gels used as superabsorber materials in diapers,[5] and poly(2-hydroxyethyl methacrylate) gels used in soft contact lenses.[21]

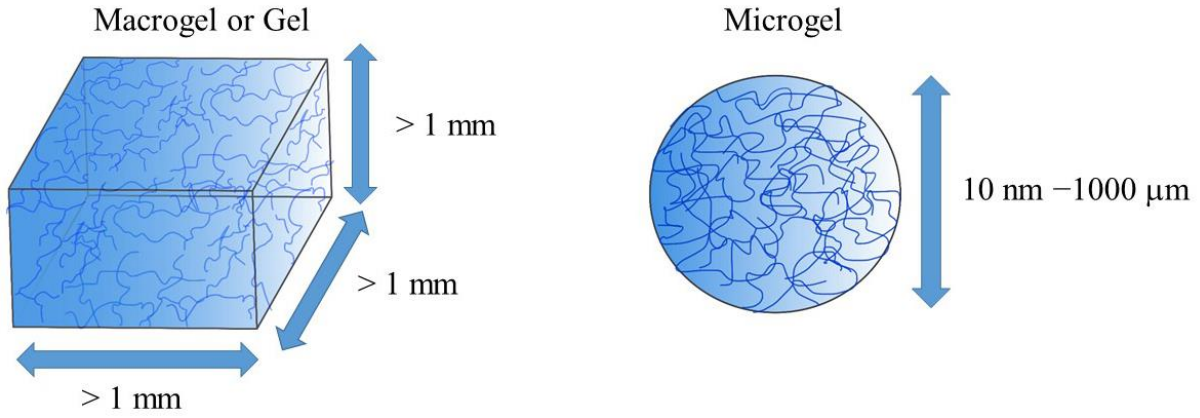

Figure 1.1. Illustration of an above-millimeter-sized macrogel (left) and of a spherical microgel with size ranging from a few nanometers to several hundreds of micrometers (right).

1.1.2 Synthesis of Polymer Gels and Microgels

Macroscopic polymer gels exhibiting covalent crosslinks are typically synthesized by one of the following different mechanisms: (i) copolymerization of mono- and multifunctional monomers;[22,23] (ii) crosslinking of linear polymer chains containing crosslinkable side groups;[24] (iii) end-linking of linear polymer chains functionalized with reactive end groups to multifunctional crosslinkers;[25] (iv) interconnection of star-shaped macromonomers whose arms are capped with suitable groups.[26]

Microgels can either consist of colloidal particles that exhibit sizes of 10−1500 nm and are subject to Brownian motion, or of granular-scale particles with sizes of 10−1000 μm, that are subject to gravitational sedimentation. Colloidal microgels are typically prepared by *precipitation polymerization* or by *miniemulsion polymerization* of mono and bi-functional monomers. A precipitation polymerization is carried out at conditions at which the forming oligomer chains are not soluble in the reaction mixture and therefore precipitate: subsequent clustering and growth of the precipitated oligomer chains lead to the formation of crosslinked microgel particles, as schematized in Figure 1.2.[27]

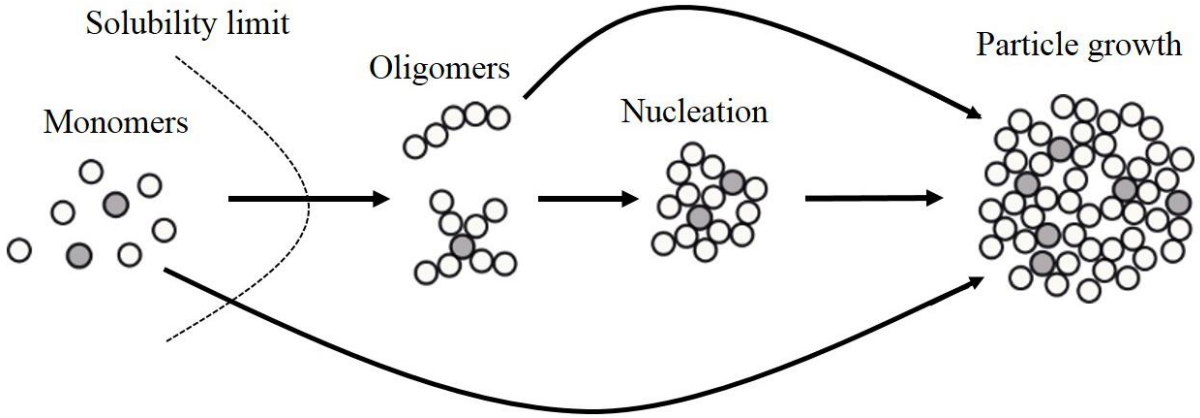

Figure 1.2. Schematic illustration of the synthesis of colloidal microgels by precipitation polymerization. White spheres represent monofunctional monomers, whereas gray spheres represent multifunctional monomers.

In a miniemulsion polymerization a solution of monomers or polymer chains is first emulsified, and subsequent initiation of the polymerization inside each droplet of the emulsion eventually leads to the gelation of such droplets and to the formation of colloidal microgels.[28] In addition, a similar droplet-templated synthetic strategy has been developed to obtain larger, granular-scale microgel particles.[29–31] For this purpose, droplets exhibiting sizes that range from a few micrometers to several hundreds of micrometers, along with very narrow size distributions, are formed by injecting two immiscible liquids into microfluidic devices. These devices usually consist either of coaxial assemblies of round and square glass capillaries glued on a glass slide,[32] or of a poly(dimethylsiloxane) (PDMS) elastomer permanently sealed on a glass slide.[33] The simplest and most common type of microfluidic device contains two inlet microchannels meeting at a junction that leads into a common outlet microchannel. In the droplet-templated synthesis of microgels, a solution of monomers or crosslinkable polymer chains (dispersed phase) is injected into the first inlet channel, whereas another immiscible fluid (continuous phase) is injected into the second inlet channel. At the junction, droplets are formed by flow-focusing of

the dispersed phase exerted by the continuous phase, as shown in Figure 1.3; these droplets act as templates for the subsequent gelation achieved by crosslinking polymerization of the monomers or of the polymer chains within them, as also shown in Figure 1.3. Besides the experimental set up described above, more complex microfluidic devices and synthetic strategies have been exploited to prepare functional microgel particles with different morphologies, such as hollow particles,[34,35] core–shell microgels[36] and anisotropic Janus microgels[37] (Figure 1.3).

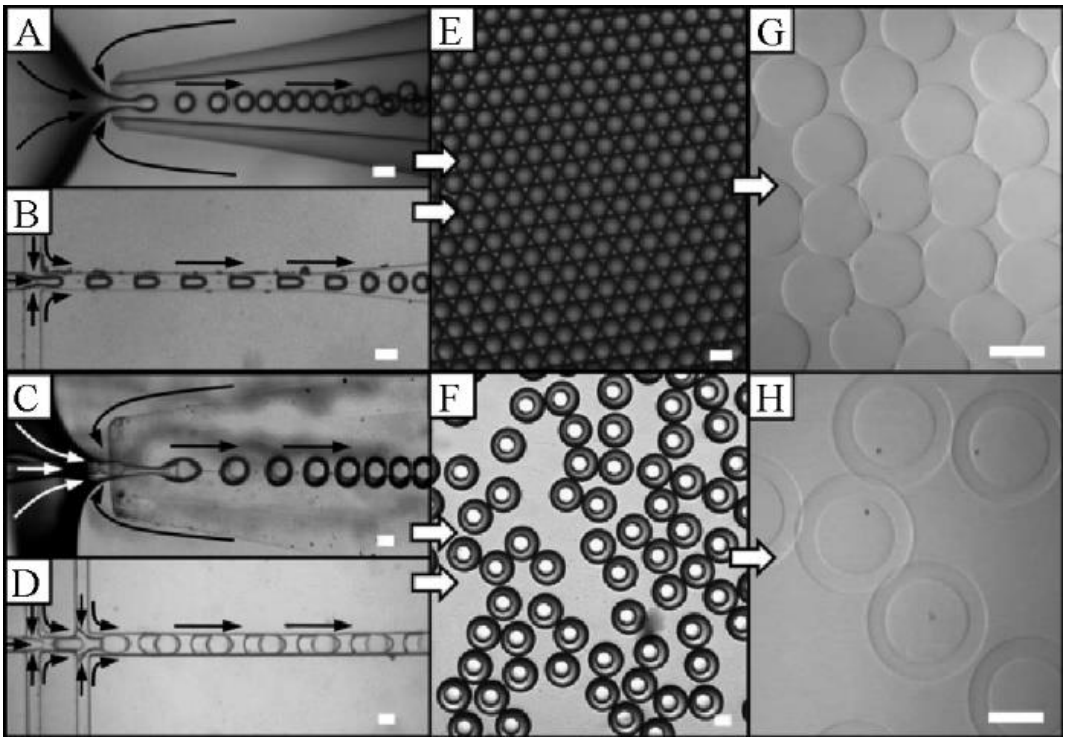

Figure 1.3. Synthesis of granular-scale microgel particles by droplet-templated polymerization in glass capillary (A,C) and PDMS elastomer (B,D) microfluidic devices; E) single emulsion droplets; F) double emulsion droplets; G) granular-scale microgels resulting after gelation of the droplets in (E); H) hollow microgels resulting from the double-emulsion templates in (F). All scale bars denote 50 mm. Reproduced with permission from ref. 31. Copyright John Wiley & Sons 2013.

1.1.3 Poly(*N*-isopropylacrylamide) Gels

Poly(*N*-isopropylacrylamide) (pNIPAm) is a polymer that is well-known for its responsiveness to temperature variations in water. This thermo-responsiveness has been investigated in the 1960s by Heskin and Guillet:[38,39] pNIPAm is a flexible, water-soluble coil at temperatures below its *lower critical solution temperature* (LCST) of ≈ 32 °C, whereas it undergoes a transition from coil to globule and then precipitates at temperatures above its LCST. The thermo-responsiveness of pNIPAm is due to the simultaneous presence of hydrophilic amide groups and hydrophobic isopropyl groups in the polymer, as shown in Figure 1.4. At temperatures below the

LCST, the amide groups interact strongly with water through hydrogen bonding. By contrast, at higher temperatures, the hydrogen bonds are broken, water becomes a poor solvent and phase separation occurs. As a result of this change in the solubility of their constituent polymer chains, crosslinked pNIPAm gels undergo a sharp transition from highly swollen networks at temperatures below the LCST, to shrunken networks at temperatures above the LCST.[39–42] This transition, denoted as the *volume phase transition*, is accompanied by large expelling of water from the polymer network at temperatures at which pNIPAm is hydrophobic, and to a large water uptake at temperatures at which pNIPAm is hydrophilic.

Linear pNIPAm chains are typically synthesized by free-radical polymerization of *N*-isopropylacrylamide (NIPAm), initiated by reduction of ammonium persulfate (APS) in the presence of tetramethylethylenediamine (TEMED), which accelerates the rate of production of free radicals.[39] Functionalization of pNIPAm can be achieved by copolymerization of NIPAm and of a comonomer that contains the desired functional group; this strategy has been exploited to label pNIPAm with fluorescent dyes or to insert photo-reactive crosslinkers in the polymer.[36,43] Another method to synthesize pNIPAm chains exhibiting additional functionality is the copolymerization of NIPAM with *N*-acryloxysuccinimide (NASI) or *N*-(methacryloxy)succinimide (MASI), followed by nucleophilic addition of an amino-functionalized molecule and by elimination of *N*-Hydroxysuccinimide. This strategy allows several copolymers exhibiting different functionalities but very similar distributions of molecular weights to be synthesized starting from a single batch of p(NIPAM-*co*-NASI) or p(NIPAM-*co*-MASI) chains.[44–46]

Crosslinked pNIPAm gels are commonly synthesized by free-radical copolymerization of NIPAm and *N*,*N*′-methylenebis(acrylamide) (BIS), as shown in Figure 1.4.[39]

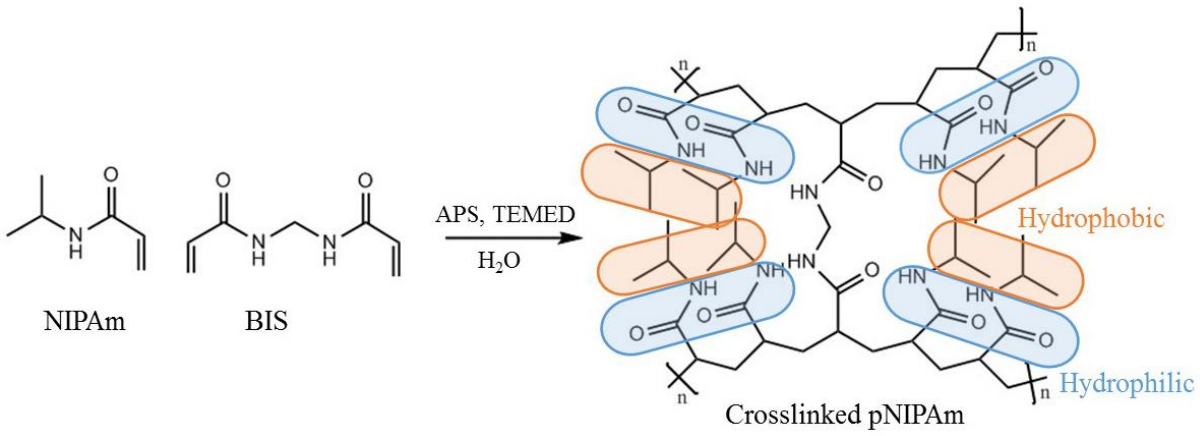

Figure 1.4. Synthesis of crosslinked pNIPAm by free-radical copolymerization of NIPAm and BIS in water, initiated by the reduction of APS in the presence of TEMED. The hydrophilic and the hydrophobic functional groups of pNIPAm are marked with blue and orange, respectively.

PNIPAm gels have been also prepared by irradiation of solutions of NIPAm with γ-rays, which simultaneously induces polymerization and crosslinking.[47] A more complex way to synthesize pNIPAm gels with better control of their nanostructure is the crosslinking of linear pNIPAm chains containing crosslinkable side groups. Following this strategy, Seiffert et al. synthesized pNIPAm gels by UV irradiation of semidilute aqueous solutions of linear pNIPAm chains containing dimethylmaleimide (DMMI) moieties randomly distributed along the chains, in presence of thioxanthone disulfonate (TXS) as triplet photosensitizer;[35,36] upon irradiation of p(NIPAm-*co*-DMMI) chains, the DMMI moieties dimerize,[48–50] leading to crosslinking of the chains and to gelation of the polymer solutions, as illustrated in Figure 1.5.

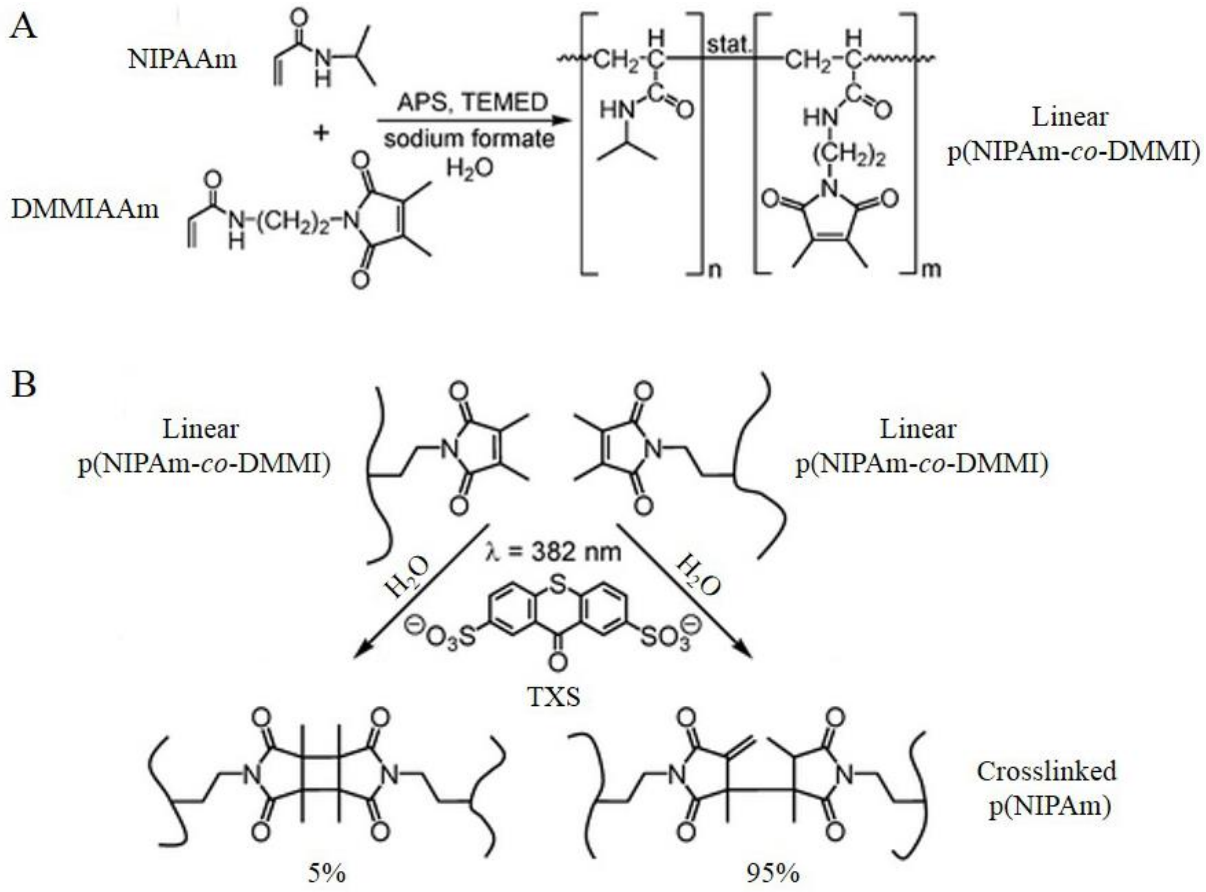

Figure 1.5. Synthesis of crosslinked pNIPAm gels by photo-crosslinking of linear pNIPAm chains containing crosslinkable DMMI moieties. (A) Copolymerization of NIPAm and (dimethlymaleimide)ethylacrylamide (DMMIAAm), initiated by the addition of APS and TEMED; sodium formate is used to control the size of the obtained chains. (B) UV-induced crosslinking of linear p(NIPAm-*co*-DMMI) chains in aqueous solution. The dimerization of DMMI is mediated by a triplet sensitizer, thioxanthone-disulfonate (TXS). Two isomeric types of dimers are formed, each of them constituting a covalent crosslinking junction between the pNIPAm chains. Adapted with permission from ref. 35. Copyright Royal Society of Chemistry 2010.

Colloidal-scale pNIPAm microgels exhibiting sizes of 100−1500 nm and narrow size polydispersity are typically prepared by precipitation polymerization, as explained in section 1.1.2. The synthesis of colloidal pNIPAm microgels was first reported by Pelton et al.,[51] and usually involves precipitation copolymerization of NIPAm and BIS at temperatures of 60−70° C, initiated by thermal decomposition of potassium persulfate or ammonium persulfate. In the first synthesis procedure reported by Pelton, the growing microgel particles were colloidally stabilized by electrostatic repulsion originating from sulfate groups introduced by the initiator.[52] Later on, a charged surfactant such as sodium dodecyl sulfate (SDS) was added to the reaction mixture to further stabilize the growing particles and thus to achieve better control of the final size of the microgels.[53,54] By contrast, if precipitation polymerization is performed in presence of an electrolyte, the microgels are destabilized, such that their final size increases with the ionic strength of the reaction media.[55] Pelton's synthesis procedure for colloidal pNIPAm microgels has been widely exploited and implemented: in this context, the copolymerization of NIPAm and BIS with a third co-monomer allowed the synthesis of ionic microgels with controlled charge density,[56−60] along with the conjugation of microgels to biomolecules, and with the labeling with fluorescent dyes.[60,61] Moreover, NIPAm was also copolymerized with a more hydrophobic or with a more hydrophilic monomer to shift the volume phase transition of the obtained microgels to lower or to higher temperatures than in the case of plain pNIPAm microgels.[62−65]

Granular-scale pNIPAm microgels exhibiting sizes of 10−1000 μm and low polydispersity have been prepared by droplet-templated polymerization in microfluidic devices, as explained in section 1.1.2.[29,66,67] For this purpose, an aqueous solution of NIPAm, BIS and APS is emulsified in an immiscible fluid, in which a small amount of TEMED is dissolved. Once water-in-oil droplets are formed, TEMED diffuses into them, thereby accelerating the reduction of APS: this initiates a free-radical polymerization inside the droplets, leading to gelation of these droplets and to the formation of microgels. The size of the obtained microgels is controlled by the size of the droplet templates, which can be tuned by varying the size of the microchannels in which the droplets are formed, along with varying the relative flow rates of the dispersed and of the continuous phases.[32] Furthermore, Seiffert et al. synthesized granular-scale pNIPAm microgels by emulsification and subsequent UV-induced gelation of solutions of linear p(NIPAm-*co*-DMMI) chains in microfluidic devices.[35−37] The microgel particles obtained with this procedure were found to exhibit a more homogeneous nanostructure in comparison to microgels formed by free-radically initiated copolymerization of monomers, as investigated by static light

scattering and NMR spectroscopy.[68] Moreover, this strategy was exploited to prepare pNIPAm microgels exhibiting different functionalities and morphologies by UV-induced crosslinking of polymer chains containing photo-crosslinkable groups, along with additional functional groups.[36,37]

1.2 Nanostructural Heterogeneity in Polymer Gels

1.2.1 Origin and Characterization of Heterogeneity in Polymer Gels

In a crosslinked polymer network, the strands between two crosslinking junctions define the network *meshes*, and the equilibrium end-to-end length of the strands defines its *mesh size,* typically $\xi = 1-10$ nm. However, most polymer networks, in particular those obtained by free-radical crosslinking copolymerization, exhibit a marked degree of nanostructural heterogeneity, manifested in form of an inhomogeneous spatial distribution of crosslinks,[69–72] as illustrated in Figure 1.6. This crosslinking heterogeneity leads to a broad distribution of network strand lengths, such that the polymer network displays a *distribution* of mesh sizes rather than exhibiting a unique, single mesh size. In addition to this distribution of chain lengths, most polymer networks display topological and connectivity defects such as dangling chain ends, chains forming closed loops, and crosslinker–crosslinker shortcuts, as also shown in Figure 1.6.

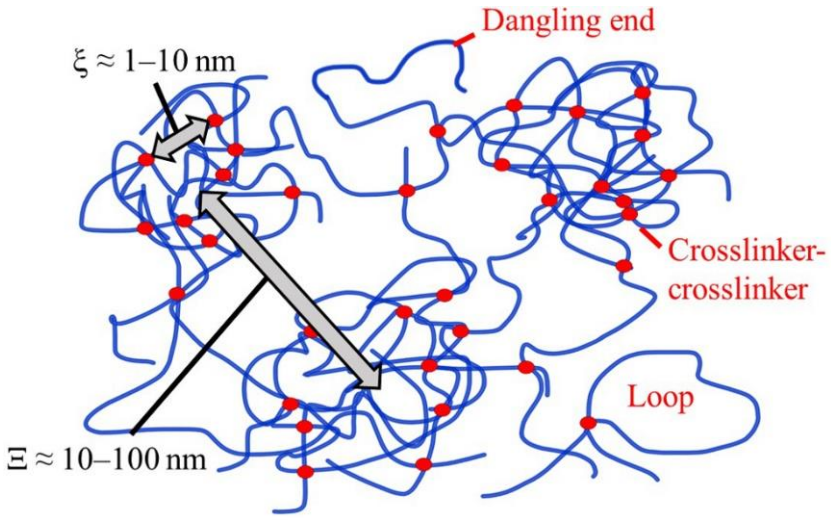

Figure 1.6. Schematic of a polymer network exhibiting inhomogeneous crosslinking density and connectivity defects. The short arrow marks a typical mesh size, $\xi \approx 1-10$ nm, whereas the long arrow indicates the typical length scale of spatial variation of the crosslinking density, $\Xi \approx 10-100$ nm. Reproduced from ref. 73. Copyright Royal Society of Chemistry 2015.

Furthermore, the spatial inhomogeneity of a polymer network increases when the network is swollen in a solvent:[74–76] this is because upon swelling, local loosely crosslinked domains expand more than local densely crosslinked domains, and this effect causes additional pronounced fluctuations in the spatial profile of the polymer segmental density and of the concentration of crosslinking junctions, as illustrated in Figure 1.7.

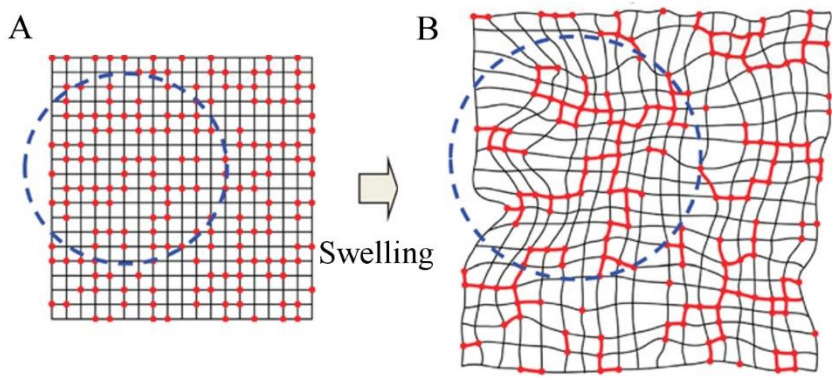

Figure 1.7. Schematic of A) randomly distributed crosslinking junctions (red dots) in a deswollen polymer network and B) the same polymer network swollen in a good solvent. Highly crosslinked local domains (red segments) swell less than the rest of the network, leading to pronounced static spatial fluctuations of the polymer concentration. Reproduced with permission from ref. 77, copyright Nature Publishing Group 2011, previously modified from ref. 74,copyright American Chemical Society 1988.

It was found that the crosslinking density is particularly inhomogeneous in polymer networks obtained by free-radical crosslinking copolymerization of bi- and multi-functional monomers in solution. This is a consequence of the mechanism of network formation: during the early stage of a crosslinking copolymerization, chain cyclization and local multiple crosslinking lead to the formation of nanogel clusters, as shown in Figure 1.8.[4,78–81] At higher conversion, macroscopic gelation occurs by rather loose interconnection of these clusters to a continuous, space-filling polymer network that therefore displays pronounced spatial concentration fluctuations on a length scale of 10–100 nm, as also illustrated in Figure 1.8.

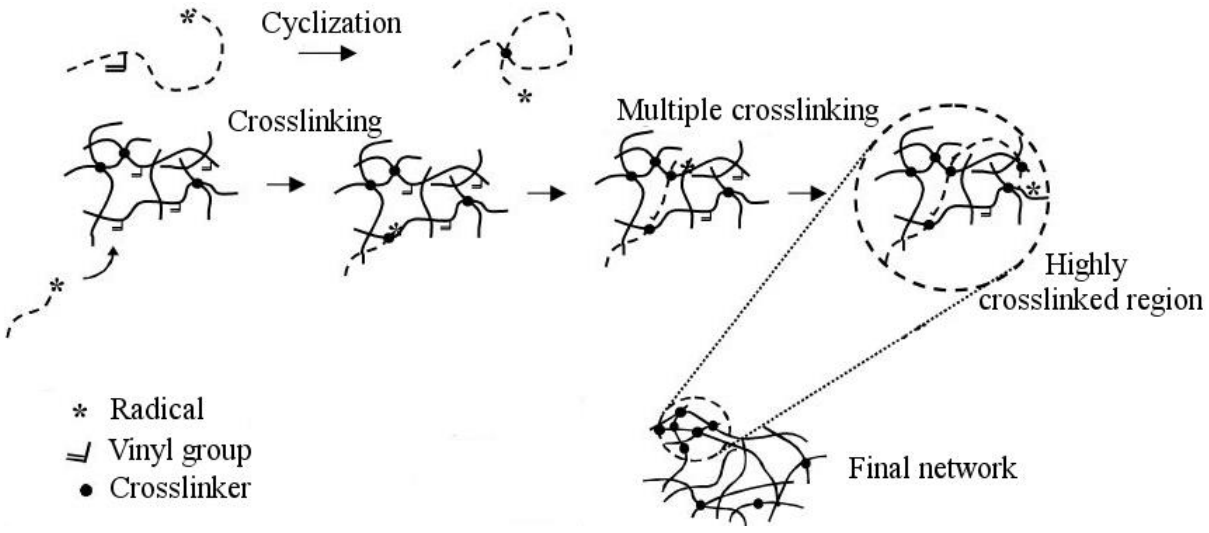

Figure 1.8. Cyclization and multiple crosslinking reactions in free-radical crosslinking copolymerization, leading to local highly crosslinked domains (area inside the dotted circle) in the final network. Adapted with permission from ref. 81. Copyright Elsevier 2003.

Thus, the extent of heterogeneity of a polymer gel depends on the polymerization mechanism and on the reaction conditions. In polymer gels obtained by free-radically initiated copolymerization of monomers, nanostructural heterogeneity increases with increasing ratio of crosslinker to monomer in the pre-gel solution,[81] and with incresing crosslinker reactivity.[82,83] This is because cyclization and multiple crosslinking reactions are more probable if the crosslinker concentration is higher during the reaction and if the crosslinker reacts faster than the main monomer. On the contrary, if the crosslinker concentration in the pre-gel solution is kept constant and the monomer concentration is increased, the probability of multiple crosslinking reactions decreases, and more homogeneous gels are formed.[84,85] Moreover, the extent of inhomogeneity of polymer gels is lower if the polymerization occurs in a good solvent, while it is more pronounced in gels polymerized in close-to theta solvents, because in a theta solvent the nanoscopic gel clusters formed in the early phase of a polymerization are unswollen, such that their volume fraction is smaller than it would be in a good solvent.[86,87] Hence, a higher conversion of the polymerization is needed for the nanogels to eventually percolate to a space-filling network, which then displays more pronounced concentration fluctuations.[84] For this reason, if the synthesis of crosslinked polymers with an upper critical solution temperature (UCST) occurs at temperatures higher than its UCST, the extent of inhomogeneity of the resulting polymer network decreases with increasing preparation temperature.[86] For the opposite case of polymers with a lower critical solution temperature (LCST) that lays above the reaction temperature, the inhomogeneity of the resulting polymer network increases with increasing polymerization temperature.[84,86,87]

The spatial inhomogeneity of polymer gels has been extensively investigated by means of NMR spectroscopy,[68,88–92] atomic force microscopy (AFM),[93–95] optical,[96,97] x-ray[98] and electron[99–101] microscopy, in addition to light[82,84,102–108], small angle x-ray (SAXS),[109,110] and neutron scattering (SANS).[75,111–115] The scattering of a polymer gel is due to fluctuations of its local polymer concentration, which are reflected by fluctuations of the gel refractive index. These fluctuations are the sum of thermal, time-dependent concentration fluctuations due to Brownian motion (ergodic contribution), and of static, time-independent concentration fluctuations that are a consequence of the inhomogeneous crosslinking density of the network (non-ergodic contribution).[116] To investigate the structural inhomogeneity of polymer networks by scattering methods, it is necessary to separate the static from the dynamic contribution to the measured scattering intensity. This is usually done by assuming the dynamic fluctuations to be

equivalent to those of a corresponding uncrosslinked polymer solution: subtracting the scattering intensity of an uncrosslinked polymer solution from that of a corresponding crosslinked polymer gel yields an excess scattering intensity that solely reflects the static concentration fluctuations of the polymer gel. Evaluation of this excess scattering intensity with the model of Debye and Bueche[117–120] allows two characteristic parameters to be derived: the *static correlation length* of the inhomogeneous polymer network density, Ξ, and the root-mean-square fluctuation of the refractive index, $\langle \delta\mu^2 \rangle^{1/2}$, which can be converted into the root-mean-square fluctuation of the concentration, $\langle \delta c^2 \rangle^{1/2}$, by use of the refractive index increment, $d\mu/dc$.[84] According to the model of Debye and Buche, the excess scattering intensity, R_{ex}, is given by

$$R_{ex}(q) = (4\pi K\, \Xi^3 \langle \mu^2 \rangle)/ (1+q^2\, \Xi^2)^2$$

where q is the scattering vector $q = 4 \sin(\theta/2)/ \lambda$, and $K = 8\pi^2\mu^2\, \lambda^{-4}$, where θ is the angle between the incident and the scattered radiation, and λ is the wavelength of the incident radiation. Alternatively, the scattering intensity of a gel can be decomposed into static and dynamic contributions by dynamic scattering methods, such as dynamic light scattering (DLS): if DLS measurements are performed at different sample positions, the measured scattering intensities can be split into position-independent scattering contributions arising from thermal concentration fluctuations (ergodic contribution) and position-dependent scattering contributions deriving from static concentration fluctuations (non-ergodic contribution), as illustrated in Figure 1.9.[106,116,121,122]

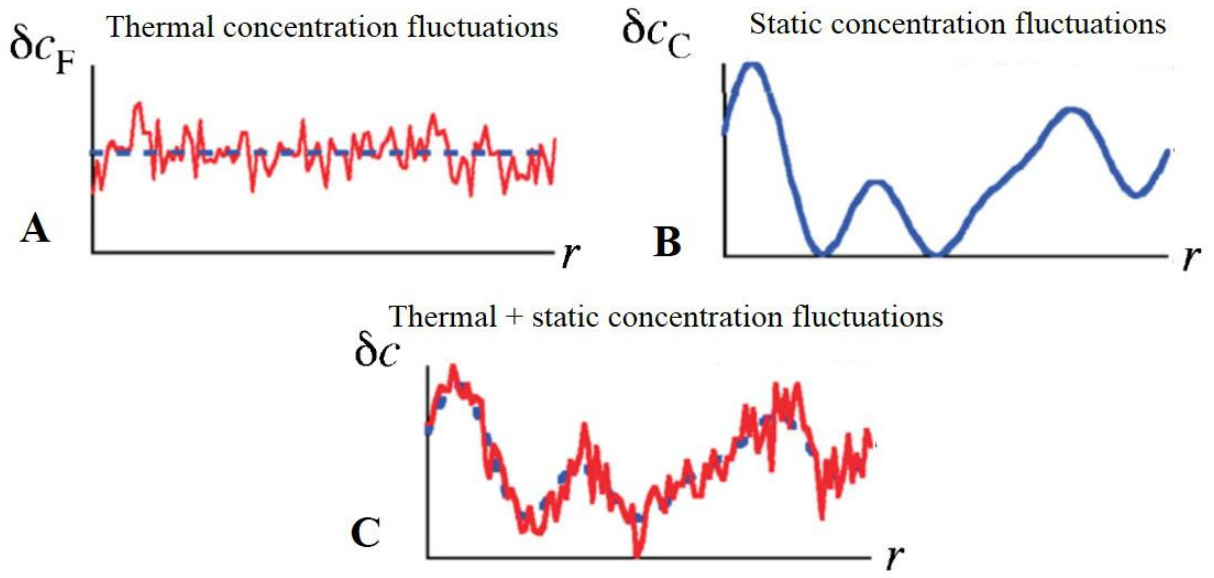

Figure 1.9. Concentration fluctuations in a polymer gel, as a function of the position on the sample: (A) thermal fluctuations due to Brownian motion (ergodic contribution); (B) static fluctuations due to frozen inhomogeneities (non-ergodic contribution); (C) superposition of the two. Adapted with permission from ref. 77. Copyright Nature Publishing Group 2011.

Besides scattering methods, atomic force microscopy has also been used to study the morphology of polymer gels.[93–95] In this technique, a cantilever equipped either with a sharp tip or with a spherical probe is used to scan the surface of a sample. In a mode of operation often referred to as *contact mode*, the tip or the sphere are dragged across the sample surface, and either the deflection of the cantilever, or the force needed to keep it at a certain position, is measured. By contrast, in different modes of operation, often referred to as *tapping* and *non-contact* modes, the cantilever oscillates in close proximity to the surface, and variations of the oscillation amplitude due to attractive or repulsive interactions with the sample are measured.[123] To investigate polymer gels, AFM is normally used in the contact mode, allowing the stiffness of the gel surface to be probed with a spatial resolution down to a few Ångstroms.[124] AFM micrographs of heterogeneous polymer gels typically display inhomogeneous surfaces.[93–95] However, AFM measures the local stiffness of a gel sample, which is then typically used to estimate the sample's local crosslinking density and to reconstruct its surface morphology. Thus, the investigation of crosslinking heterogeneity in polymer networks by AFM relies on the assumption that there is a simple relation between the stiffness of a gel and its crosslinking density. This assumption would require each crosslinking junction of the polymer network to equally contribute to the gel stiffness; however, this is not concluded to be true by several studies, as detailed in Section 1.2.2. Thus, while AFM is a convenient technique to locally probe the mechanical properties of hydrogels,[125–127] it is less suitable to investigate their heterogeneous nanostructures.

1.2.2 Effect of Nanostructural Heterogeneity on the Elasticity of Polymer Gels

Crosslinked polymer networks composed of long flexible chains are able to sustain high levels of deformation if they are subjected to stress, and to recover their initial shape after stress removal.[128] Their elasticity was first described about 70 years ago by the statistical theory of rubber elasticity.[129–134] In this theory, each flexible chain strand of a polymer network is treated like an elastic spring with determined spring constant and equilibrium length: the most likely chain conformation is that of a random coil, whereas the most unlikely conformation is that of a fully decoiled chain. Upon deformation of the polymer network, each elastic chain decoils and thereby loses conformational freedom: as a result, an entropy-driven elastic restoring force originates. On the basis of this conceptual picture, different models were developed to describe the deformation of a polymer network. In the *affine network* model, the positions of the crosslinks are affine to the macroscopic deformation of the network.[130,135] In the *phantom network* model, only the time-averaged mean positions of the crosslinks are affine to the macroscopic

deformation.[133,134] According to these variants of the theory of rubber elasticity, the elastic shear modulus of a polymer gel, *G',* increases linearly with the concentration of its constituent elastic chains, ν, as by $G' = \nu\, k_B T$ in the affine model or by $G' = (1 - 2/f)\, \nu\, k_B T$ in the phantom model, where f is the functionality of the crosslinks.[130] Hence, in both these models, the main contribution to elasticity is the number of elastic network chains, while the distribution of network chain lengths is considered to be monodisperse.

In contrast to this simple picture, the experimentally measured elastic properties of many rubbers and gels, such as their response to applied shear and uniaxial compression and extension, showed deviations from the predictions of the theory of rubber elasticity.[136–138] These deviations were attributed to network topological defects[137–140] and to complex chain conformation statistics.[141,142] To account for these deviations, the concept of *effective elastic chains* was introduced.[139,140,143] In this concept, effective elastic chains (ν_{eff}) are defined as chains that actively contribute to the elasticity of the network by deforming and storing elastic energy, in contrast to dangling chains or chains forming loops, which are not elastically active. In addition, several studies by Mark et al. showed that, besides these network defects, a broad distribution of chain lengths affects the elasticity of a polymer network, such that the theory of rubber elasticity does not always apply to inhomogeneous gels. In this context, Mark et al. observed that bimodal polymer networks containing large fractions of very short chains randomly mixed with small fractions of much longer chains had improved stability if subjected to elongation and rupture.[144–148] This has been explained with the limited extensibility of the short chains, and with the fact that stretching of such chains above a certain limit would require variation of the bonding angles between the monomers in the backbone. Moreover, Mark et al. also prepared bimodal networks that consisted of highly crosslinked domains randomly distributed on a soft, loosely crosslinked background.[149,150] In contrast to the first type of bimodal networks, the networks with segregated crosslinking density displayed lower stability to elongation and lower storage moduli. This findings were explained by considering that if the chains between two or more crosslinkers are too short to be deformed and to store elastic energy, as it might happen inside the highly crosslinked nanodomains, several crosslinkers within those must be regarded to act as a single crosslinking supernode with low ability for elastic energy storage.[149,151] Further studies have shown that the elastic modulus of a gel, as determined by rheology, decreases with increasing degree of inhomogeneity in the gel, as determined by light scattering.[85] In addition, the elastic moduli of polymer gels obtained by uncontrolled polymerization are generally lower than what would be expected from their content of crosslinker on basis of the statistical theory

of rubber elasticity. This decrease can be quantified by the efficiency of crosslinking of the gel, defined as ν_{eff}/ν, where ν is the ideally achievable crosslinking density calculated from its content of crosslinker, whereas ν_{eff} is the actual density of elastically active crosslinks, inferred from the shear elastic moduli of the gels according to the statistical theory of rubber elasticity. For heterogeneous gels prepared by uncontrolled free-radically initiated copolymerization of monomers, the efficiency of crosslinking is 0.1–20%,[81,82,85] while for less heterogeneous polymer networks obtained by crosslinking of pre-polymerized linear chains functionalized with crosslinkable moieties, or by end-linking of linear polymer chains with multifunctional monomers or oligomers, the efficiency of crosslinking is 3–70%.[49,107,152,153] These previous works suggest that both the presence of inelastic network defects such as loops and dangling ends and the formation of highly crosslinked local domains in polymer networks might lead to a marked decrease of the crosslinking efficiency in heterogeneous gels.

1.2.3 Effect of Nanostructural Heterogeneity on the Permeability of Polymer Gels

A prominent area of application of polymer gels is that of polymeric membranes in separation techniques[6–10] or for the encapsulation and controlled release of additives such as drugs.[11–16] In both these areas of use, the gel permeability is of central relevance. This quantity is directly related to the mesh size of the polymer gel. If additives are smaller than the polymer network meshes, their self-diffusion in a gel is not affected by the polymer network. In this case, the diffusion coefficient of the additives, D, is related to the friction acting on them, F, by the Einstein relation, $D = k_B T / F$. In the case of spherical additives, the friction was calculated by Stoke, and the diffusion coefficient is given by the Stoke-Einstein relation, $D = k_B T / 6\pi\eta R$, where η is the viscosity of the solvent.[154,155] By contrast, if the additives are polymer chains smaller than the polymer network meshes, their self-diffusion has been described by the *Rouse model*.[156] According to this model, each of the N beads of a polymer chain is characterized by an own independent friction coefficient, F_{Bead}, and the total friction acting on the chain is given by the sum of all frictions coefficients acting on its beads. As a result, the Rouse diffusion coefficient of the polymer chain is $D_{Rouse} = k_B T / (F_{Bead} N) \sim M_w^{-1}$, where M_w is the molecular weight of the diffusing chain. In the opposite case of additives that are larger than the polymer network meshes, two different scenarios are observed. If the additives are rigid, their diffusion through the polymer network is hindered: thus, the additives either cannot penetrate in the gel matrix, or they are permanently immobilized in its interior. By contrast, if the additives are flexible polymer chains, they can creep or “reptate” through the polymer network even if their own size is larger than the size of the network meshes. This mechanism of motion has been

described by De Gennes in his *reptation* theory.[157–162] In this theory, the self-diffusion of a linear flexible macromolecule within a polymer network is modeled to proceed as a worm-like motion of a chain confined in a tube-like region, as shown in Figure 1.10. This tube is either defined by temporary topological constraints, such as chain entanglements, or by permanent topological constraints, such as crosslinking junctions. On time scales shorter than a characteristic *reptation time*, τ_{Rep}, the diffusing chain only fluctuates inside the tube-like region, while on longer time scales, the chain diffuses along and eventually out of the tube. The reptation theory predicts that the reptation time depends on the molecular weight of the reptating chain as $\tau_{Rep} \sim M_w^3$, while the diffusion coefficient of the chain is $D \sim M_w^{-2}$.

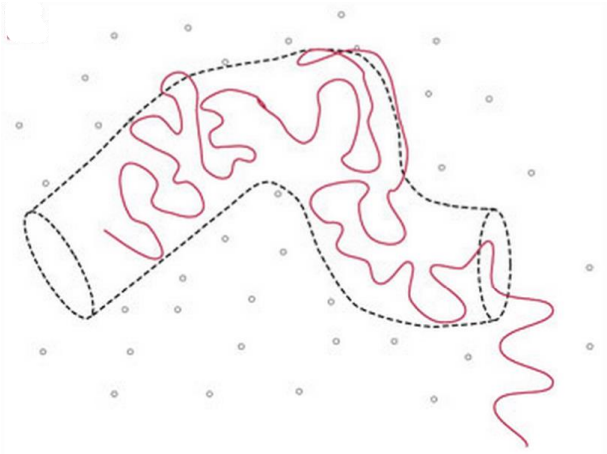

Figure 1.10. Concept of the reptation theory: a linear polymer chain fluctuates in a tube-like region defined by topological constraints. In a polymer melt, the topological constraints are entanglements with other polymer chains, whereas in a crosslinked polymer network, the topological constraints are represented by crosslinking junctions. Reproduced with permission from ref. 163. Copyright Nature Publishing Group 2008.

In the reptation theory, the crosslinking junctions of a polymer network are assumed to be fixed obstacles, and variations in their spatial distribution are neglected. In contrast to this simplification, deviations of experimental results from the predictions of the reptation theory, for example, in view of the scaling of D with M_w, have been attributed to polymer network heterogeneities.[164,165] In addition, theoretical studies suggest that the diffusion of reptating chains in heterogeneous media is slower than predicted by the reptation theory, because the diffusing chains can be subject to entrapment in energetically favorable regions.[166–169] This is particularly relevant if the size of the diffusing chains is similar to the size of these regions and therefore to the length scale of heterogeneities in the polymer network matrix.[164] However, these studies focus on the mobility of synthetic polymers or biomacromolecules such as DNA diffusing in polymer networks of different chemical composition, and simulations show that

the diffusivity of such heteropolymer samples is slower than in case of homopolymer chains reptating within chemically identical matrixes.[170] In contrast, other investigations report experimental estimates of the diffusion of both homopolymer and heteropolymer tracer chains to be in accordance with the predictions of the reptation theory.[171,172] The preceding survey shows that no clear picture has been developed to date. In particular, no comprehensive experimental studies focusing on the self-diffusion of polymer tracer chains in model polymer network matrixes with well-defined heterogeneity are known.

Nevertheless, the self-diffusion of flexible polymer chains through polymer gels of the same chemical composition has recently been investigated by fluorescence recovery after photobleaching (FRAP) by Seiffert, Susoff and Opperman.[172,173] For this purpose, polymer chains were labelled with a fluorescent dye and embedded within a non-fluorescent polymer network. At a certain time, the mobile fluorescent chains were bleached by irradiation with a laser at high intensity that locally destroys the fluorophores, leading to a local attenuation of the fluorescence intensity in the bleached region, as shown in Figure 1.11. Subsequently, the fluorescence intensity of the sample was recorded with spatial and temporal resolution by confocal fluorescence microscopy, as also shown in Figure 1.11.

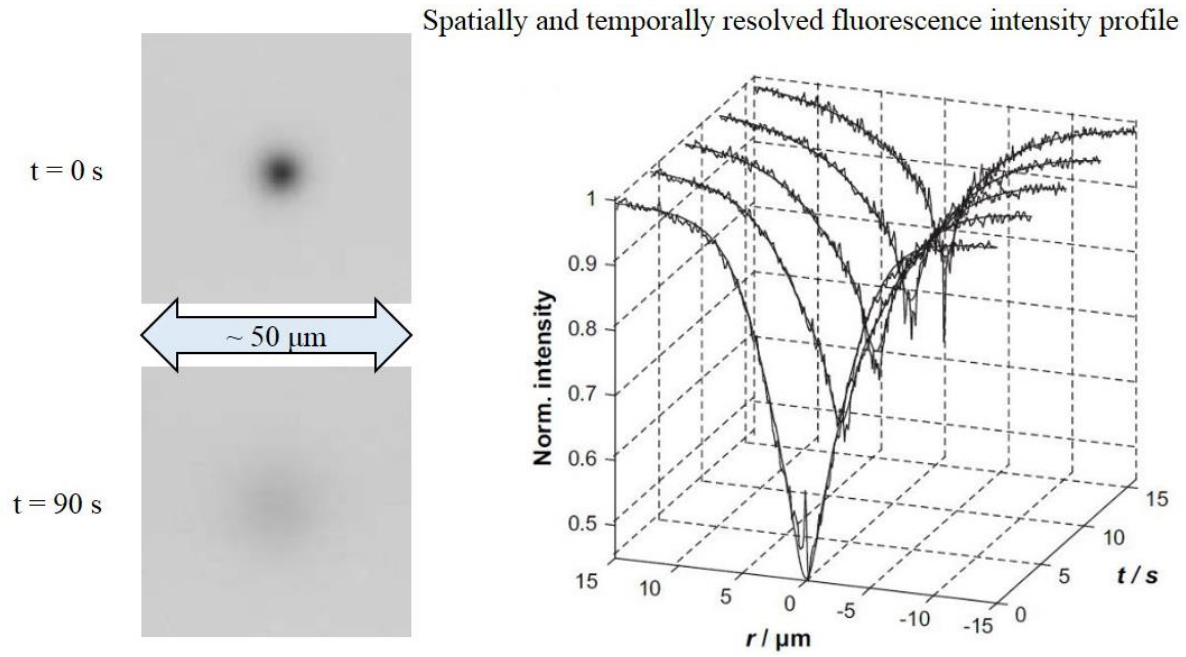

Figure 1.11. Confocal fluorescence microscopy images (left) and fluorescence intensity profile (right) recorded in a FRAP experiment as a function of the time. At the time t = 0 s, one spot of the sample is bleached by irradiation with a laser at high intensity; the formed pattern smears with increasing observation time *t*, due to the diffusion of the fluorophores. Adapted with permission from ref. 173 (copyright Elsevier 2008) and from ref. 174 (copyright John Wiley & Sons 2005).

The local attenuation of the fluorescence intensity smears out with increasing observation time due to the diffusive exchange of bleached and unbleached fluorophores, characterized by an ensemble of diffusion coefficients. Thus, the analysis of the measured fluorescence intensity profiles with a diffusion model developed by Hauser, Seiffert and Opperman,[174–176] yields distributions of diffusion coefficients for the fluorescent polymer chains in the polymer network.

Part of section 1.2 was reproduced with permission from ref. 73. Copyright The Royal Society of Chemistry 2015.

1.3 Packed Suspensions of Microgel Particles

1.3.1 The Limiting Case of Hard Spheres

Hard spheres (HS) are defined as rigid, impenetrable and incompressible spherical particles.[177] Two hard spheres interact through an infinite repulsive pair potential, $U(r) = \infty$, if the interparticle distance, r, is smaller or equal to the sum of their radii, $\sigma = R_1 + R_2$; in the opposite case of $r > \sigma$, $U(r) = 0$.[177] In the late 1950s, simulations predicted the phase diagram for a suspension of monodisperse spheres interacting through a hard-sphere repulsive potential.[178,179] These simulations revealed that a suspension of hard spheres undergoes a transition from liquid-like to solid-like mechanics upon increase of the particle volume fraction, φ. According to these simulations, a suspension of monodisperse hard spheres has the disordered structure of a fluid up to the particle volume fraction $\varphi_{freeze} = 0.49$, whereas for $0.49 < \varphi < 0.55$ a fluid and an ordered crystal phase coexist, and for $0.55 < \varphi < 0.74$ the whole suspension exhibits a crystalline ordered structure, as shown in Figure 1.12. The volume fraction of 0.74 is the maximal volume fraction reachable in a suspension of monodisperse incompressible spheres, and corresponds to the volume fraction of *hexagonal close packing*, φ_{cp}. By contrast, in suspensions of hard spheres with polydispersity larger than ≈ 8%, a different scenario is observed: crystallization is suppressed and, instead, an amorphous solid-like phase is formed at the volume fraction of $\varphi_g = 0.58$; this phase is denoted as *colloidal glass*,[180] in analogy with molecular glasses. A colloidal glass consists in a disordered, dynamically arrested state that persists up to the maximal volume fraction of a completely random packing of spheres, referred as the *random close packing,* $\varphi_{rcp} = 0.64$,[181]

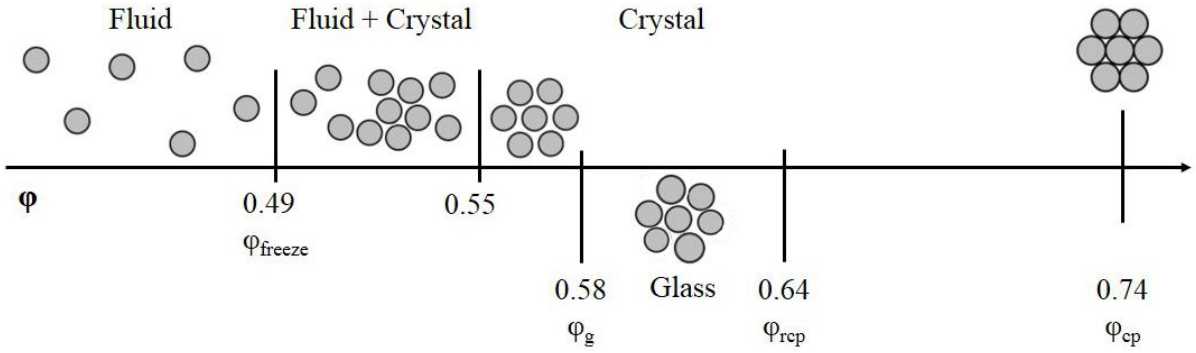

Figure 1.12. Phase diagrams of suspensions of hard spheres. In the phase diagram above the horizontal arrow, the spheres are monodisperse and crystallize upon increase of the volume fraction above φ_{freeze}. By contrast, in the phase diagram below the horizontal arrow, the spheres are polydisperse and the suspension undergoes a transition from fluid to glass at the volume fraction φ_g; φ_{rcp} is the maximum particle volume fraction of a completely random packing of spheres; φ_{cp} is the packing fraction of hexagonal close packing. Modified with permission from ref. 182. Copyright Elsevier 2002.

as also shown in Figure 1.12.

In the 1980s, experiments by Pusey and van Hagen reproduced for the first time the predicted phase diagram for hard spheres using colloidal poly(methyl methacrylate) (PMMA) particles, which were sterically stabilized by a thin layer of poly(hydroxystearic acid) to minimize attraction due to Van der Waals forces.[183,184] Since then, PMMA particles have been used in many experimental studies as model systems for hard spheres.[185–191] Moreover, if the particles used in these experiments are large enough, the fluid, the crystal and the glassy phases of their suspensions can be directly observed by optical microscopy, as shown in Figure 1.13.[192]

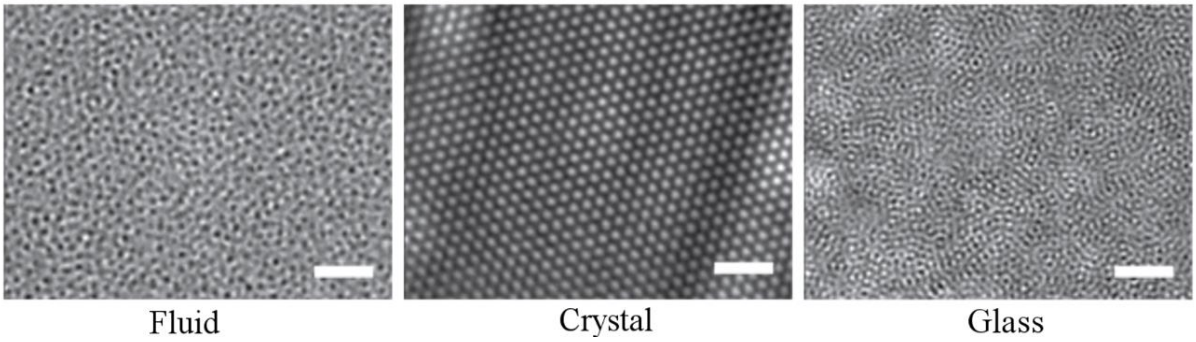

Figure 1.13. Microscopic images of suspensions of hard spheres in the fluid, in the crystal and in the glass phase, obtained over an observation time of 10 s. The scale bars represent 10 μm. Modified with permission from ref. 192. Copyright Annual Reviews 2012.

1.3.2 Tuning the Softness of Colloids from Hard to Soft Spheres

In contrast to hard spheres, microgels are soft, deformable particles; their softness is determined by the softness of their repulsive pair potential, which is defined as $U(r) = \varepsilon (\sigma/r)^n$, where ε sets the energy scale, n controls the stiffness of the potential ($1/n$ is the softness), and r and σ are the interparticle distance and the sum of two particle radii, respectively, as already defined for hard spheres (see section 1.3.1).[193] In the limit of $n \rightarrow \infty$, the soft repulsive pair potential corresponds to the repulsive pair potential of hard spheres. Several types of colloids have been classified according to their softness, which increases from hard spheres to polymer coils, going through emulsions, microgels and star-shaped polymers, as illustrated in Figure 1.14.[194] In addition to hard spheres, suspension of soft particles also undergo a liquid-to-solid transition upon increase of their particle volume fraction. Moreover, soft particles have the ability to deform, and in some cases to interpenetrate and to deswell; thus, the determination of their volume fraction in a suspension is not trivial.[195] For this reason, suspensions of soft particles are better characterized by the particle *packing fraction,* $\zeta = d\,V_d$, where d is the number density of particles per unit volume and V_d is the volume of a fully swollen single particle in the dilute limit.[66]

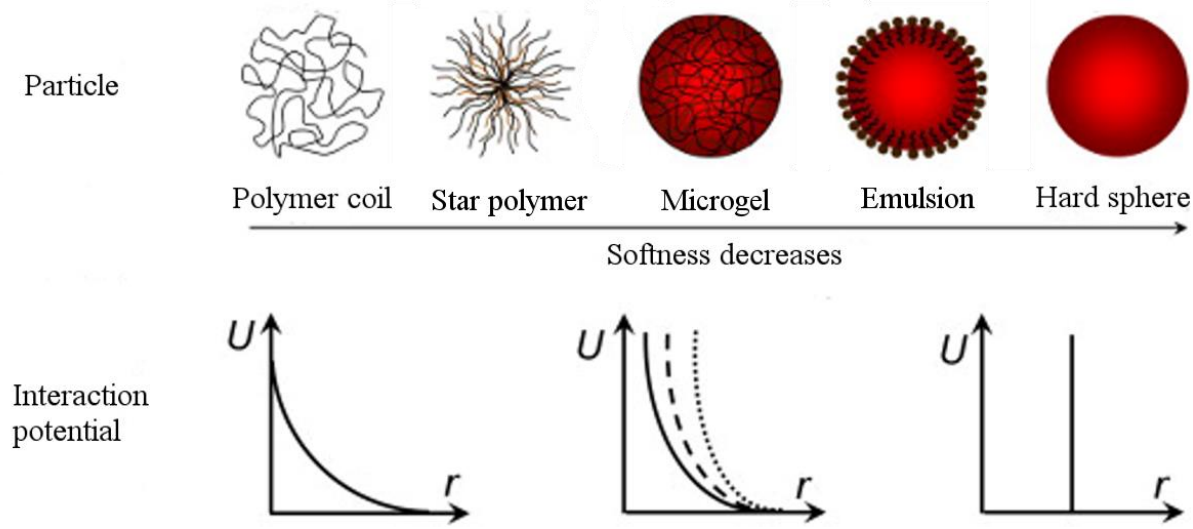

Figure 1.14. Classification of different types of colloids according to the softness of their repulsive pair potential. This softness decreases starting from polymer coils and going to star-shaped polymers, microgels, emulsions and finally to the limit case of hard spheres, as pictured above. The shape of the corresponding repulsive pair potentials is pictured below: dashed and dotted lines illustrate the variability of this potential with the particle morphology. Adapted with permission from ref. 194. Copyright Elsevier 2014.

The packing fraction of a suspension of soft particles can be calculated by knowledge of the total mass concentration of particles in the suspension, c, and of the mass concentration of a single particle in the dilute limit, c_P, as $\zeta = c/c_P$. If particle interpenetration and deswelling are absent, a space-filling packing of particles is characterized by $\zeta = 1$. By contrast, in suspensions of interpenetrating or deswollen particles, ζ can reach values much larger than 1.[66,196]

In most experimental studies on soft colloids, crystallization is not observed. Instead, suspensions of colloidal spheres subject to Brownian motion undergo a *colloidal glass transition.* This transition has been explained with the concept of each particle being dynamically trapped in a cage composed by the surrounding particles.[187,188,197] A further increase of the packing fraction of a suspension of soft particles above random close packing leads to a dense state in which particles are deformed and form polyhedral facets at contact; this second type of transition is referred as the *jamming transition,* and depends on contact forces between the deformed particles.[198–202] Suspensions of colloids have been found to undergo both glass and jamming transitions: for example, suspensions of hard spheres-like colloids undergo a transition to a glass,[203] whereas emulsion droplets first undergo a glass transition and then, upon further increase of their volume fraction, a jamming transition.[204,205] For colloidal microgel particles

interacting through soft repulsive potentials, however, no such clear picture exists. In this context, suspensions of core–shell microgels composed of a soft pNIPAm shell and a hard polystyrene (pS) core have been shown to undergo a transition to a glass,[206,207] but no universal behavior has been observed for plain pNIPAm microgels.

The liquid-to-solid transition of suspensions of colloids has been widely investigated by means of rheology,[189,190,196,206–211] microrheology,[209,212] dynamic light scattering,[184,213–216] confocal microscopy[187,188,217,218] and UV-vis spectrophotometry.[196] An attempt to determine the state diagram of suspensions of colloidal particles exhibiting different extents of softness has been recently made by Vlassopoulos and Cloitre.[194] According to this classification, which is based on experimental studies, the state diagram of suspensions of microgels does not strongly differ from that of hard spheres, as shown in Figure 1.15.

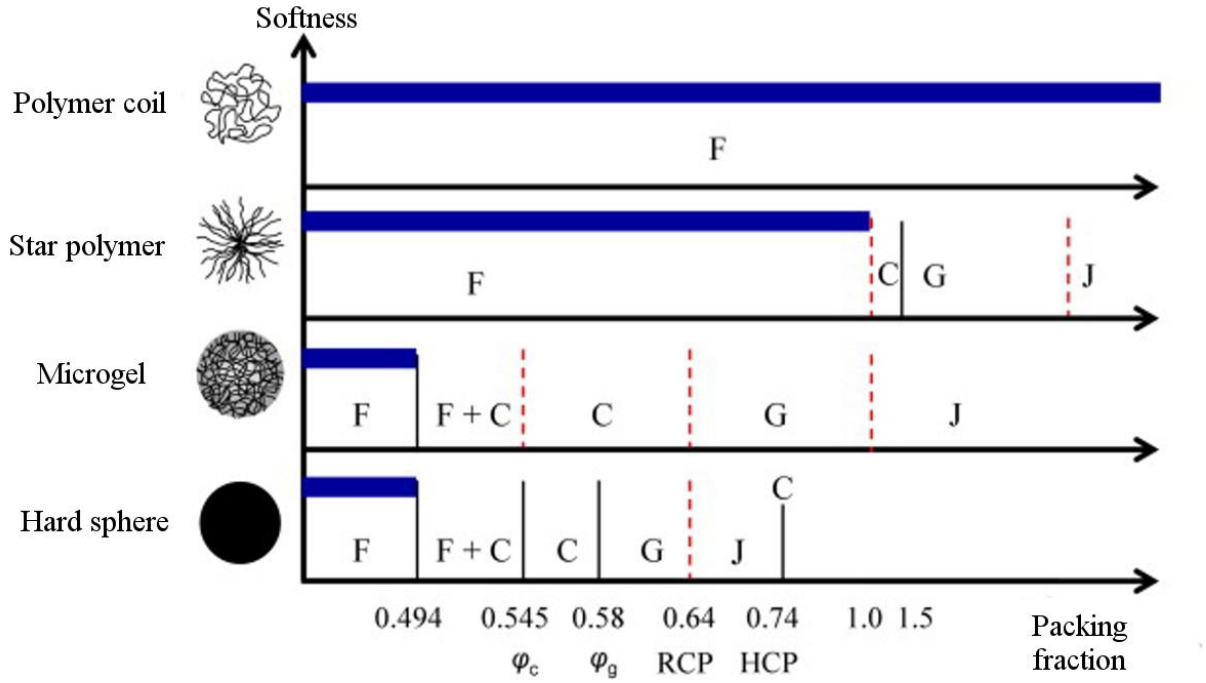

Figure 1.15. State diagrams of suspensions of colloids with varying softness, as a function of the particle packing fraction. The softness of the colloids increases from hard spheres to polymer coils, going through microgels and star-shaped polymers. The letters refer to different states: F) stands for *fluid*, F+C) denotes the coexistence of *fluid* and *crystal*, C) denotes a *crystal* phase, G) stands for *glass* and J) refers to a *jammed* state. RCP and HCP are the volume fraction of random close packing and of hexagonal close packing for hard spheres, respectively. Adapted with permission from ref. 194. Copyright Elsevier 2014.

Suspensions of these two types of particles exhibit the same fluid, crystal, glassy and jammed states, with the exception that the packing fraction of the glass transition is slightly upshifted

from 0.58 for hard spheres to 0.64 for microgel particles, and that the packing fraction of the jamming transition is upshifted from 0.64 for hard spheres to 1 for microgels, as also shown in Figure 1.15. In contrast to this simplified classification, existing studies denote large variance of the packing fraction at which the glass and jamming transitions of suspensions of microgels occur. The state diagram of microgel suspensions shown in Figure 1.15 is based on experimental studies on colloids that exhibit different sizes and morphologies, such as plain pNIPAm microgels,[210,219] PMMA microgels,[220] and core–shell microgels made of a hard polystyrene core and of a soft pNIPAm shell.[221] These results are in accordance with other investigations on core–shell pS–pNIPAm microgels;[190,207,211] these particles have been used as model systems to study the colloidal glass transition, in agreement with theoretical predictions of the Mode Couple Theory (MCT),[207,221] because their packing fraction can be elegantly controlled by temperature variations, which cause the swelling or the shrinking of the thermosensitive pNIPAm shell. However, other investigations on suspensions of soft pNIPAm microgels indicate that the liquid-to-solid transition of such suspensions occurs at much larger effective packing fractions, $\zeta \approx 2-3$ or even $\zeta \approx 9$, reachable only by strong deswelling of the microgels.[215,222] Moreover, the liquid-to-solid transition was found to be more gradual for suspensions of soft microgels than for hard spheres: in suspensions of hard spheres, a small increase of the particle packing fraction causes significant slowing of the suspension structural relaxation and therefore a sharp liquid-to-solid transition, whereas in suspensions of soft spheres, this dynamic arrest stretches over a wide range of packing fractions.[215,223] Furthermore, it was recently observed that the state diagram of suspensions of colloidal poly(vinylpyridine) microgels strongly depends on the particle softness, such that suspensions of very soft, loosely crosslinked microgels remain fluid at all packing fractions investigated (up to 10), whereas suspensions of highly crosslinked, stiff microgels undergo transition to a glass at $\zeta \approx 0.6$.[196] This is in agreement with theoretical studies that predict the packing fraction of the glass transition of soft colloids to increase with the particle softness,[193] and to other experimental work suggesting the existence of a relation between the packing fraction of the glass transition and the bulk elastic moduli of core–shell microgels composed of a pNIPAm core and of a poly(*N*-isopropylmethacrylamide) shell.[224] In addition, recent simulations by Ikeda, Berthier, and Sollich suggest that not only the softness, but also the particle size affect the occurrence of the liquid-to-solid transition of suspensions of soft colloids.[204] According to these simulations, the ratio between the thermal energy and the elastic energy of a suspension of soft particles is a key parameter for the understanding of the glass and jamming transitions of soft particulate materials.

The combination of soft and hard interactions in suspensions containing both soft and hard colloids allows the macroscopic properties of these composite materials to be studied and to be tuned on a microscopic length scale. For this purpose, several types of binary colloidal mixtures of particles exhibiting different softness have been investigated in the last years, as for example mixtures of star-shaped polymers with polymer coils,[225] and mixtures of star-shaped polymers of different sizes and softness.[226,227]

1.3.3 Rheology of Dense Microgel Suspensions

The liquid-to-solid transition of particle suspensions can be followed by shear rheology.[228] In a small angle oscillatory shear experiment, a small sinusoidal strain, $\gamma(t) = \gamma_0 \sin(\omega t)$, is applied to the sample, which is placed between two parallel plates, between a plate and a cone, or between two concentric cylinders, depending on the experimental set up chosen, as shown in Figure 1.16. In a solid, the stress caused by this shear, the *shear stress* $\tau(\gamma)$, is proportional to the shear strain as $\tau(\gamma) = G\,\gamma(t) = G\,\gamma_0 \sin(\omega t)$, where G is the shear elastic modulus of the solid. By contrast, in a fluid, the shear stress is proportional to the shear velocity, $d\gamma/dt$, as $\tau(\gamma) = \eta\, d\gamma/dt\,(t) = \eta\,\gamma_0\,\omega\cos(\omega t)$, where η is the viscosity of the fluid. In a viscoelastic material, the shear stress is not in phase with the applied strain, as also shown in Figure 1.16, and is given by $\tau(\gamma) = \gamma_0 [G'(\omega)\sin(\omega t) + G''(\omega)\cos(\omega t)]$, where G' is the *storage* or *elastic modulus* and G'' is the *loss* or *viscous modulus* of the material. If $G' >> G''$, the material exhibits solid-like mechanics, whereas if $G' << G''$, liquid-like mechanics is observed. In a small angle oscillatory experiment, $G'(\omega)$ and $G''(\omega)$ are measured at different shear oscillation frequencies, ω, allowing the response of the material to be probed on different time scales. At each oscillation frequency, the material is probed on a time scale $t = 2\pi/\omega$, with t typically ranging from ≈ 100 ms to several minutes.

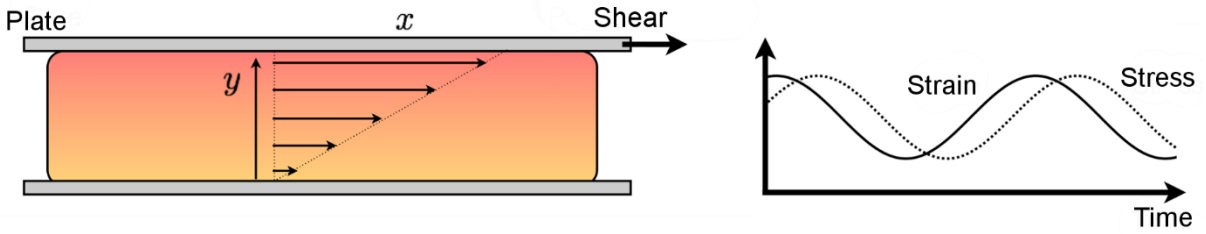

Figure 1.16. A viscoelastic sample is placed between two parallel plates and subjected to a shear applied by the upper plate (left); the stress caused by shearing is not in phase with the strain (right). Adopted from ref. 229.

The evolution of the elastic and loss moduli of suspensions of colloids approaching the glass transition has been widely investigated by small angle oscillatory rheology.[190,207,208,210,211,230,231] If a suspension is fluid, the loss modulus, *G*'', is larger than the storage modulus, *G*', on the whole range of typically probed time scales. With increasing particle packing fraction, the storage modulus increases; the approach of the liquid-to-solid transition is characterized by *G*'= *G*'', as shown in Figure 1.17 A. A further increase of the particle packing fraction in the suspension leads to the progressive formation of a plateau of the storage modulus, G_P', and to the emergence of a minimum of the loss modulus, as shown in the Figures 17 B, C and D.

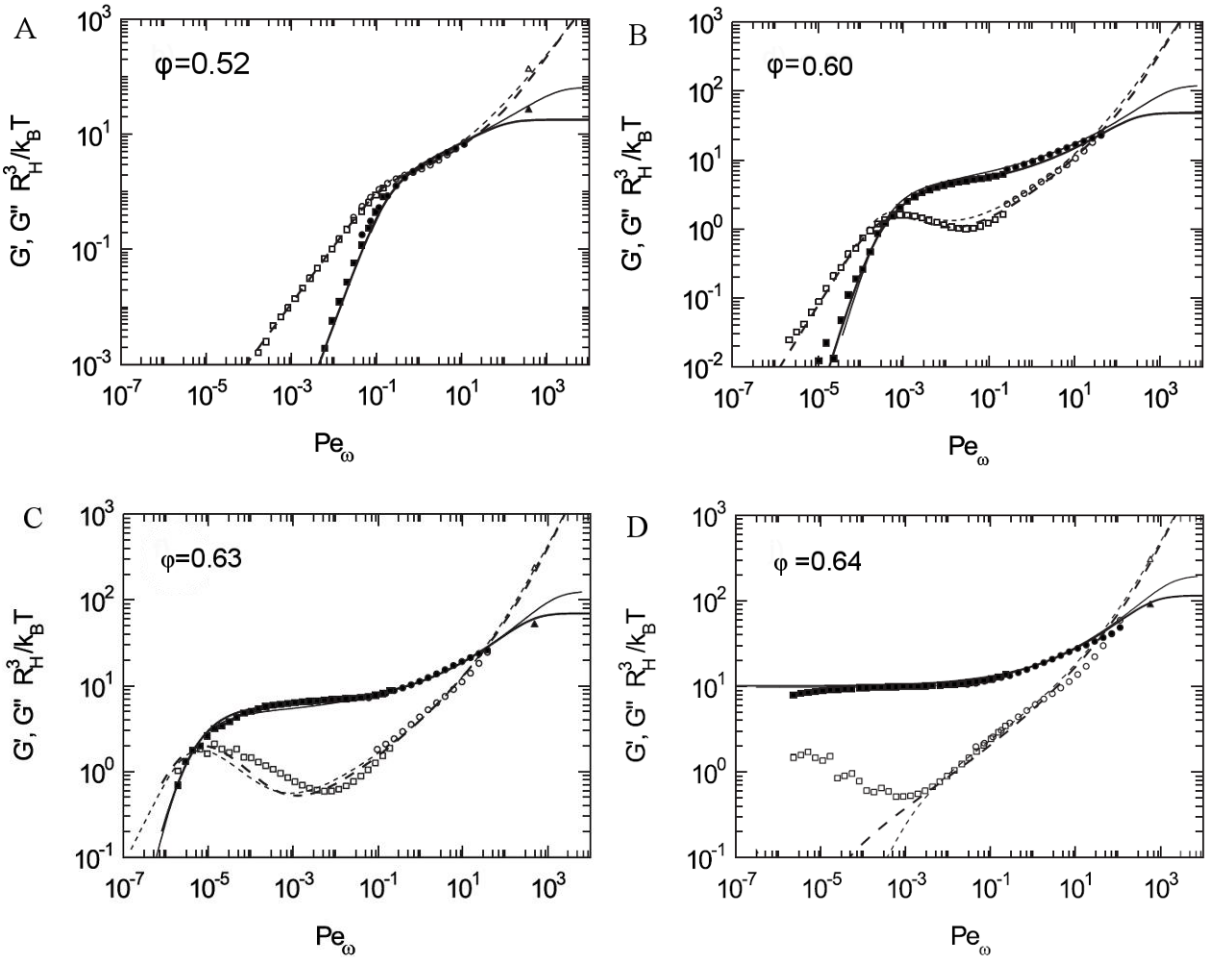

Figure 1.17. Storage modulus, *G*', (full symbols) and loss modulus, *G*'', (open symbols) of suspensions of core–shell pS-pNIPAm microgels, normalized by the particle thermal energy, k_BT/R^3, and reported as a function of $Pe_\omega = \omega\tau_B$, where ω is the oscillation frequency of the shear, and τ_B is the Brownian time of the microgels. The volume fraction of the microgel suspension increases from φ = 0.52 to φ = 0.64 going from Figure A to D. In this range of packing fractions, the suspension undergoes the colloidal glass transition, marked by the formation of a plateau of *G*' and by the appearance of a minimum of *G*''. Adapted with permission from ref. 207. Copyright The Society of Rheology 2009.

Experimental work by Siebenbürger et al.[207] on suspensions of core–shell pS–pNIPA microgels is shown in Figure 1.17. In these suspensions, the particle volume fraction is controlled by tuning the thickness of the thermosensitive pNIPAm shell. To account for different microgel sizes in suspensions at different packing fractions, G' and G'' are normalized by the thermal energy of the microgels, k_BT/R^3, whereas the angular oscillation frequency is multiplied by their Brownian time $\tau_B = R^3 6\pi\eta/ k_BT$, where R is the radius of the microgels and η is the viscosity of the solvent.

The glass transition has been explained with the concept of each particle being dynamically trapped in a cage composed by its surrounding particles, as illustrated in Figure 1.18.[187,188,197] Within this conceptual picture, the oscillation frequency of the $G'(\omega) = G''(\omega)$ crossover corresponds to the inverse time of particle motion out of the cage, defined as the α relaxation time τ_α (≈ lifetime of a cage), as shown in Figure 1.18. By contrast, the oscillation frequency at which G'' displays a minimum corresponds to the inverse characteristic time, τ_C, of the transition from out-of-cage (α relaxation) to in-cage particle dynamics (β relaxation), as also shown in Figure 1.18. Both τ_α and τ_C increase with increasing particle packing fraction while approaching the glass transition, with $\tau_\alpha, \rightarrow \infty$ for an ideally arrested glass. By contrast, τ_C displays a maximum corresponding to the packing fraction of the glass transition and decreases with increasing the particle packing fraction above this transition.[190,208,232] The initial increase of τ_C below the packing fraction of the glass transition is due to the slowing down of structural relaxation, while the decrease of τ_C above the packing fraction of the glass transition has been explained by progressive tightening of the cages around the particles.[190,208,232]

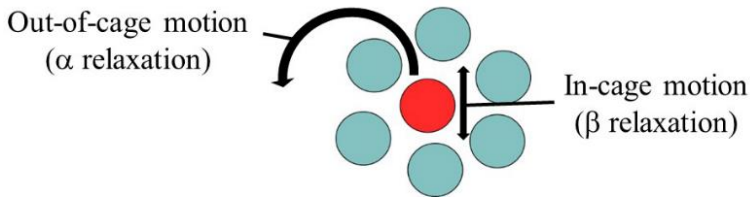

Figure 1.18. In a particle suspension approaching the glass transition, a particle is entrapped in a cage formed by the neighboring particles. The α relaxation time corresponds to the particle out-of-cage motion and to the melting of the cage; the β relaxation time is related to particle motion inside its cage.

Above the liquid-to-solid transition, the plateau value of the storage modulus, G_P' increases with the particle packing fraction as $G_P' \sim \zeta^m$, where $m = (n / 3) + 1$ and n is the stiffness of the repulsive pair potential of the particles (see section 1.2.2).[220] Thus, the measurement of G_P' of particulate materials at different particle packing fractions allows the softness of their constituent particles to be quantified. As a result, it was found that $m \approx 50$ for suspensions of

hard-sphere-like PMMA particles,[189,190] whereas $m \approx 4-7$ for core–shell pS–pNIPAM microgels,[189,190,211,233] as shown in Figure 1.19A. In contrast to this clear picture, a wide range of m values, $m \approx 3–22$, has been observed for plain pNIPAm microgels,[66,209,231,234] because these particles can be prepared within a wide range of softness, by varying both their crosslinking density and their polymer concentration.[231] This observation suggests that pNIPAm microgels are a suitable system to study the liquid-to-solid transition of particle suspensions with respect to the particle softness.

Finally, for microgel suspensions at very high packing, a different dependence of G_P' on the particle packing fraction was observed.[66,192,209] In these densely-packed microgel suspensions, the plateau storage modulus increases approximately linearly with the microgel packing fraction, as shown in Figure 1.19B for p(ethyl acrylate-*co*-methacrylic acid) microgels. The reason for two regimes observed, $G_P' \sim \zeta$ and $G_P' \sim \zeta^m$ (with $m > 1$), lies in the different microstructures of the microgel packings. At low packing, an increase of the microgel packing

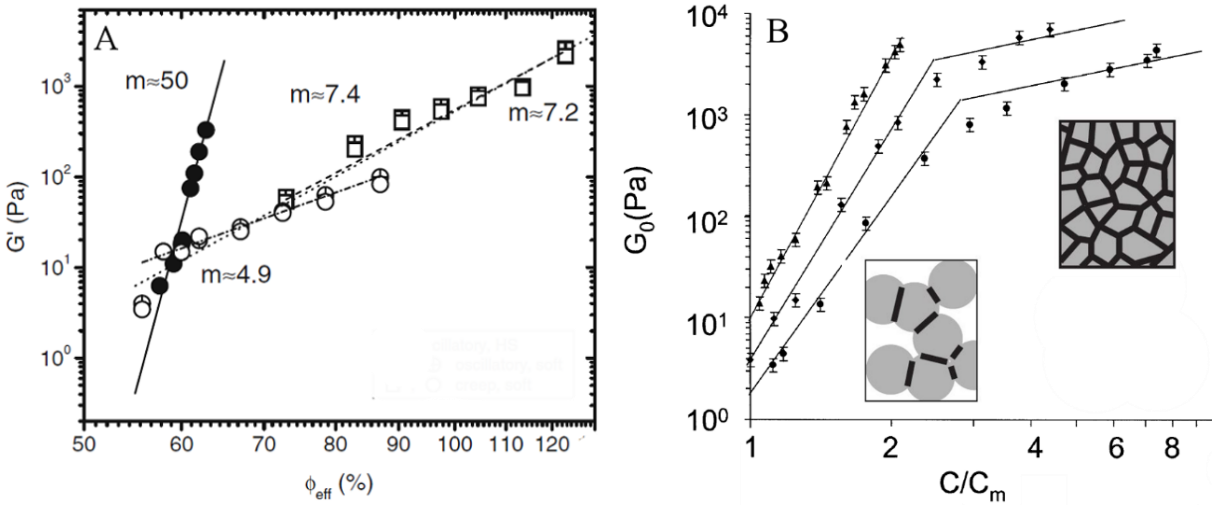

Figure 1.19. A) Plateau storage modulus, G', of PMMA microgels (full symbols) and of two different batches of core–shell pS–pNIPAm microgels (open symbols) as a function of the particle volume fraction. G' scales with φ^{50} for suspensions of hard-spheres-like PMMA microgels, while this scaling is less steep, φ^{5-7}, for suspensions of core–shell microgels made of a hard core and of a soft shell. Reproduced with permission from ref. 206. Copyright 2008 Springer. B) Plateau storage modulus, G_0' of p(ethyl acrylate-co-methacrylic acid) microgels of different softness as a function of the microgel concentration, C, normalized by the concentration corresponding to a volume fraction of $\varphi = 0.64$, C_m. At low packing, G_0' scales with C^{6-7} and the exponent of this power law decreases with increasing microgel softness. At high packing the microgels are space-filling and G_0' increases approximately linear with C. Adapted with permission from ref. 192 (copyright Annual Reviews 2012), previously modified from ref. 209 (copyright Elsevier 2003).

fraction leads to an increase of the number of contact facets between the particles: this corresponds to a sharp increase of the storage modulus, as shown in Figure 19B. By contrast, in dense, space-filling microgel packings with fixed packing geometry, also shown in Figure 19B, an increase of the microgel packing fraction solely causes the particles to deswell, such that the packing as a whole deswell similarly to macroscopic gels, resulting in an linear increase of G_P' with the density of crosslinking junctions, as assessed by the theory of rubber elasticity (see section 1.2.2).[66,129,130]

2 Scientific Goals

The physical and chemical properties of synthetic polymer gels and microgels are not only determined by the chemical composition of gels, but also by their microscopic structure. Thus, the improvement of the currently available polymer gels and the development of new types of functional gels require a deep understanding of the relation between the nanostructure of these gels and their properties. This is particularly important if the macroscopic properties of polymer gels shall be tuned by tailoring their microscopic structure. However, the preparation of polymer gels exhibiting defined and defect-free nanostructures relies on complex synthetic strategies that are in most cases incompatible with large-scale production. By contrast, polymer gels obtained by uncontrolled polymerization methods usually exhibit structural defects such as a spatial inhomogeneous crosslinking density and topological network defects. For this reason, the understanding of the impact of such nanostructural complexity on the properties of polymer gels is a central goal of polymer research. In this context, both the microscopic and the macroscopic properties of gels exhibiting nanostructural heterogeneity should be investigated, depending on the time scale and on the length scale on which these properties are relevant for a given application.

The first part of this thesis aims at elucidating the impact of nanostructural heterogeneity on the physical properties of macroscopic polymer gels. For this purpose, the mechanics and the dynamics of polymer gels exhibiting well-defined extents of heterogeneity are investigated, with a focus on the relation between structural heterogeneity and these physical properties, measured both on a microscopic and on macroscopic length scale, as shown schematically in Figure 2.1. PNIPAm gels exhibiting different extents of purposely added crosslinking heterogeneity are prepared by photo-crosslinking of linear polymer chains containing a low amount of photo-crosslinkable groups, mixed either with linear chains containing a much larger amount of photo-crosslinkable groups, or with densely pre-crosslinked microgel particles additionally functionalized with photo-crosslinkable groups. As a result, polymer gels are obtained that exhibit crosslinking heterogeneity on a length scale that is determined by the size of the precursor polymer chains and microgels, as confirmed by static light scattering. The effect of nanostructural heterogeneity on the permeability of these gels to macromolecules is investigated by measuring the self-diffusion of linear pNIPAm tracer chains within the gels by fluorescence recovery after photo-bleaching (FRAP). In addition, the global, macroscopic elasticity of these gels, measured by shear rheology on an experimental length scale of several millimeters, is compared

with the local, microscopic elasticity of the same heterogeneous gels, measured on a nanometric and on a micrometric experimental length scale by atomic force microscopy.

In another conceptual approach, macroscopic polymer gels exhibiting inhomogeneous crosslinking density are modelled by densely packed suspensions of pNIPAm microgel particles. These microgel packings exhibit macrogel-type mechanics, because the microgel packing geometry is fixed. Thus, dense heterogeneous microgel packings containing major fractions of soft, loosely crosslinked microgels and minor fractions of stiff, densely crosslinked microgels mimic the structure of inhomogeneous macroscopic gels that exhibit densely crosslinked network domains randomly distributed on a loosely crosslinked background. The effect of purposely added structural heterogeneity on the elasticity of these dense microgel packings is studied in this work by shear rheology, whereas their permeability to linear polymer tracer is investigated by FRAP.

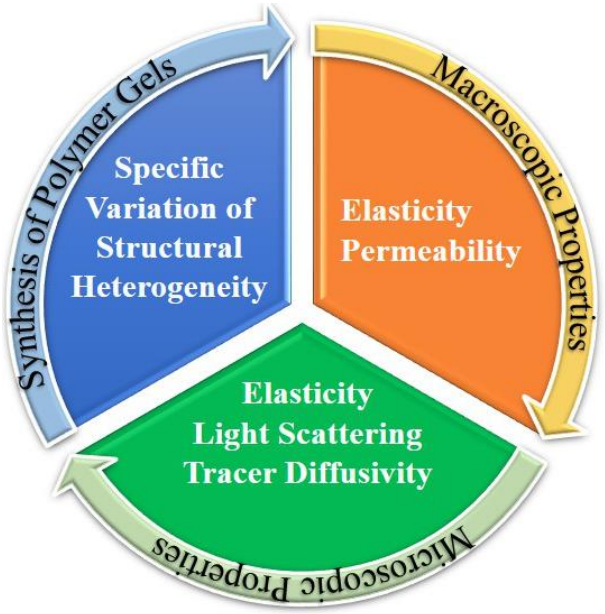

Figure 2.1. Concept of this thesis: polymer gels are prepared with determined extents of nanostructural heterogeneity and their physical properties are studied on macroscopic and a microscopic experimental length scales.

Suspensions of colloidal particles undergo a transition from viscous, liquid-like to elastic, solid-like mechanics upon increase of the particle packing fraction. In suspensions of colloids where Brownian motion is relevant, this transition is of entropic origin and is termed *colloidal glass transition*. If, in contrast, Brownian motion is negligible and the liquid-to-solid transition depends on contact forces between the particles, this transition is called *jamming*

transition. Suspensions of colloidal hard spheres undergo a glass transition at the packing fraction $\zeta \approx 0.58$, whereas jamming occurs at $\zeta \approx 0.64$. For microgel particles interacting through soft repulsive potentials, however, no such clear picture exists: in contrast, existing studies denote large and seemingly contradictive variance of the packing fraction at which the liquid-to-solid transition of suspensions of soft microgels occurs.[196,215,219–224]

The second part of this thesis aims at clarifying the apparent broad variance of occurrence of the liquid-to-solid transition of suspensions of microgels. In these studies, the liquid-to-solid transition of suspensions of pNIPAm microgels is investigated by shear rheology, with a focus on the effect of particle softness and size on the occurrence of this transition. The microgels investigated are either colloidal, sub-micrometer-sized particles subject to Brownian motion, or granular-scale, above-micrometer-sized particles subject to gravitational sedimentation. In addition, these microgels consist either of soft, loosely crosslinked particles, or of stiff, densely crosslinked particles. This allows the liquid-to-solid transition of their suspensions to be studied within a wide range of particle softness and sizes. Furthermore, microgel packings with heterogeneous structure are prepared by mixing soft microgels with stiff microgels of the same size in different particle number ratios, to study the effect of nanostructural heterogeneity on the elasticity of the obtained composite microgel packings.

3 Publications

3.1 *Tracer Diffusion in Heterogeneous Polymer Networks*

F. Di Lorenzo and S. Seiffert, *Macromol. Chem. Phys.,* **2014**, *215*, 2097–2111.
DOI: 10.1002/macp.201400317.

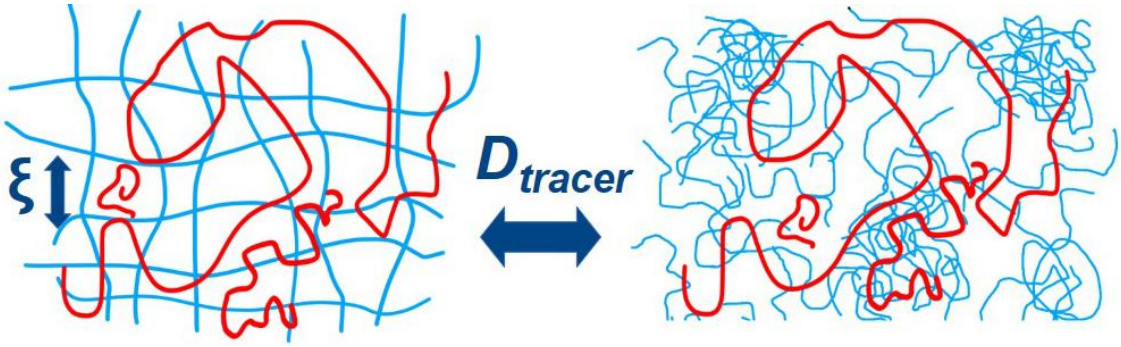

Author contributions:

F. Di Lorenzo**:** Synthesis of crosslinkable chains and microgels, labeling of polymer tracer chains, UV-vis photometry, dynamic light scattering, viscosity measurements, fluorescence recovery after photobleaching measurements and data analysis, preparation of the manuscript.

S. Seiffert: Conception and supervision of the work, labeling of polymer tracer chains, UV-vis photometry, rheology measurements under UV exposure, static light scattering measurements and data analysis, correction of the manuscript.

In this work, the self-diffusion of flexible linear pNIPAm chains in pNIPAm networks exhibiting different extents of spatial heterogeneity of their crosslinking density was investigated. Gels with just a little spatial heterogeneity were prepared by photo-crosslinking one single batch of identical polymer chains. By contrast, gels with more pronounced heterogeneity were obtained by photo-crosslinking of mixtures of two different batches of polymer chains, one with high and one with low degree of functionalization with crosslinkable groups. In addition, heterogeneous gel composites were prepared from crosslinkable polymer chains and defined fractions of pre-crosslinked microgel particles that served as doped-in domains of high crosslinking density. The extent of heterogeneity of the resulting gels was determined by static light scattering, while their shear elasticity was investigated by rheology, and the self-diffusion of fluorescent linear tracer chains within the gels was probed by fluorescence recovery after photobleaching. The outcome of these investigations is that spatial heterogeneity of a given crosslinking density in swollen polymer networks decreases their ability to store mechanical deformation energy, but has no significant impact on the above-micrometer-scale diffusivity of linear tracer chains.

3.2 *Macroscopic and microscopic elasticity of heterogeneous polymer gels*

F. Di Lorenzo, J. Hellwig, R. von Klitzing and S. Seiffert, *ACS Macro Lett.*, **2015**, *4*, 698–703. DOI: 10.1021/acsmacrolett.5b00228.

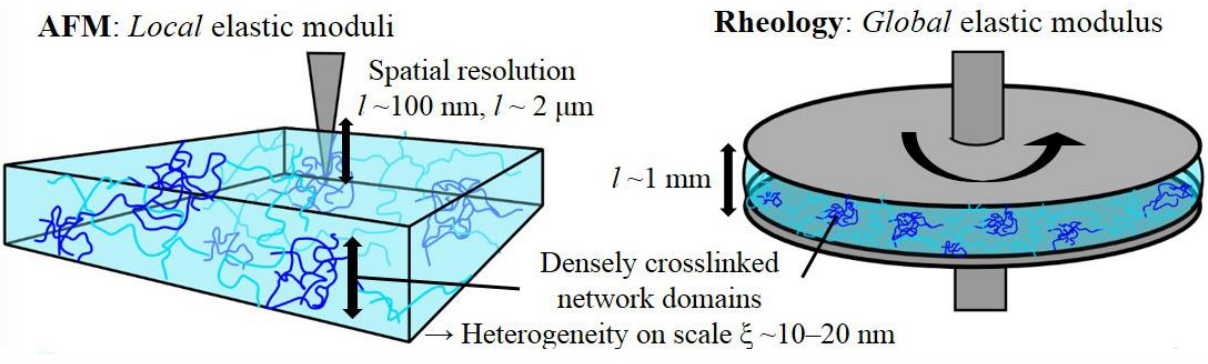

Author contributions:

F. Di Lorenzo: Synthesis of polymer gels, UV-vis photometry, preparation of the manuscript.

J. Hellwig: Atomic force microscopy measurements and data analysis, preparation of the manuscript.

R. von Klitzing: Correction of the manuscript.

S. Seiffert: Conception and supervision of the work, correction of the manuscript.

In this work, the elasticity of pNIPAm gels exhibiting different extents of crosslinking heterogeneity was investigated both on a microscopic length scale, by atomic force microscopy, and on a macroscopic length scale, by shear rheology. Atomic force microscopy was used to measure the local, microscopic Young's moduli of gel regions on a length scale close to that of the nanostructural inhomogeneities purposely added to the gels. These experiments probe the effect of network topological defects on the microscopic elasticity of gel regions with different nanostructures. By contrast, rheology experiments were performed to measure the macroscopic elastic moduli of the gels on an experimental length scale that is much larger than that of their internal structural inhomogeneities. These experiments probe both the effect of network topological defects and that of a potentially non-affine deformation of densely crosslinked gel domains. In these studies, the elastic moduli of heterogeneous gels were to found be progressively smaller if the length scale of the probed gel region exceeds the size of polymer network heterogeneities. This finding were explained with the conceptual picture of non-affine deformation of the different polymer network domains.

3.3 *Nanostructural heterogeneity in polymer networks and gels*

F. Di Lorenzo and S. Seiffert, *Polymer Chem.*, **2015**, *6*, 5515–5528.
DOI: 10.1039/C4PY01677G.

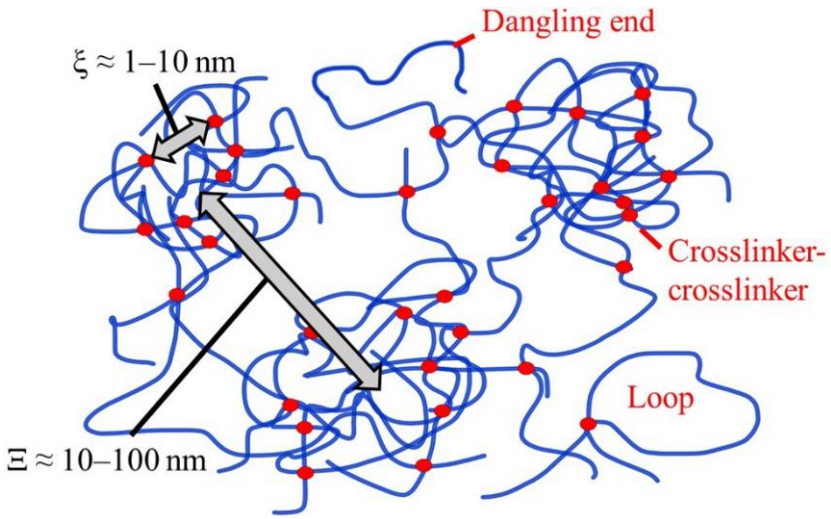

Author contributions:

F. Di Lorenzo**:** Preparation of the manuscript.

S. Seiffert: Conception of the work, correction of the manuscript.

Many polymer networks and gels display nanostructural heterogeneity in the form of spatially inhomogeneous crosslinking density, along with additional topological defects such as dangling chain ends, crosslinker–crosslinker shortcuts, and chains forming loops. In this article, existing studies on the origin of nanostructural heterogeneity in polymer gels and on the characterization of such heterogeneity by scattering techniques, microscopies, and NMR spectroscopy were reviewed. In addition, recent investigations on the impact of nanostructural heterogeneity of polymer networks on the elasticity, the swelling, and on the permeability of crosslinked polymer gels were summarized and interrelated.

3.4 *Macro- and Microrheology of Heterogeneous Microgel Packings*

F. Di Lorenzo and S. Seiffert, *Macromolecules,* **2013**, *46*, 1962–1972.

DOI: 10.1021/ma302255x.

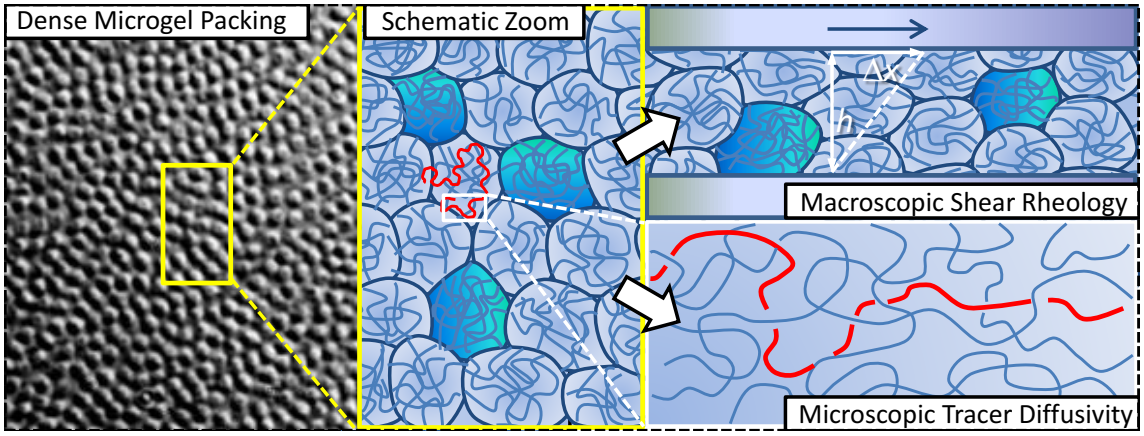

Author contributions:

F. Di Lorenzo: Synthesis of microgels, dynamic light scattering, viscosity measurements, osmotic compression, shear rheology measurements and data analysis, preparation of the manuscript.

S. Seiffert: Conception and supervision of the work, osmotic compression, polymer tracers labeling, fluorescence recovery after photobleaching measurements and data analysis, preparation and correction of the manuscript.

In this work, dense suspensions of pNIPAm microgel particles were used to model macroscopic gels. These microgel packings exhibit macrogel-type mechanics, because the microgel packing geometry is fixed. This effect provides a way to model macroscopic polymer gels with inhomogeneous nanostructure by inserting nanometer-sized spatial inhomogeneities into dense microgel packings. Following this idea, heterogeneous microgel packings were prepared by mixing major fractions of soft, loosely crosslinked microgels with minor fractions of stiff, densely crosslinked microgels. The obtained microgel packings contain densely crosslinked domains randomly distributed on a soft background, and therefore resemble the structure of macroscopic gels with inhomogeneous crosslinking density. The elasticity of these heterogeneous microgel packings was studied by shear rheology, while the microscopic mobility of flexible linear tracer polymers that diffuse through them was investigated by fluorescence recovery after photobleaching. From these studies it results that whereas the presence of densely crosslinked domains does not exhibit any systematic effect on the microscopic tracer-chain diffusivity in the heterogeneous packings, it contributes to their macroscopic shear elastic modulus.

3.5 *Particulate and continuum mechanics of microgel pastes: effect and non-effect of compositional heterogeneity*

F. Di Lorenzo and S. Seiffert, *Colloid Polym. Sci.,* **2013**, *291*, 2927–2933.
DOI: 10.1007/s00396-013-3032-8.

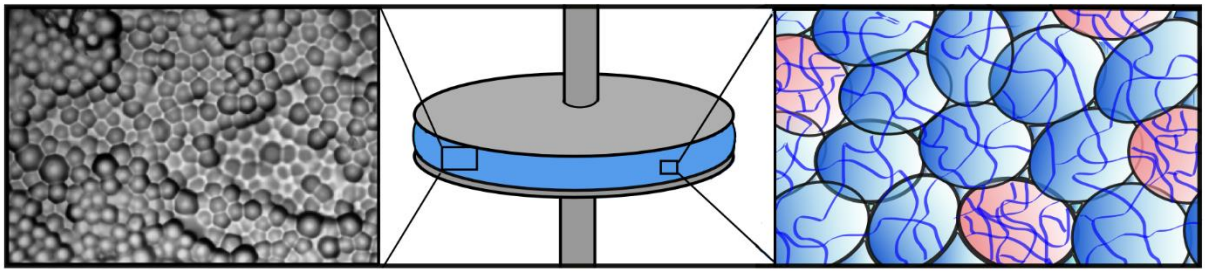

Author contributions:

F. Di Lorenzo**:** Synthesis of microgels, dynamic light scattering, viscosity measurements, osmotic compression, shear rheology measurements and data analysis, preparation of the manuscript.

S. Seiffert: Conception and supervision of the work, correction of the manuscript.

In this work, the linear viscoelasticity of packings of 1 µm-sized pNIPAm microgels particles was investigated by oscillatory shear rheology. These packings contained either solely soft, loosely crosslinked microgels, or solely stiff, densely crosslinked microgels, or both these types of microgels mixed in different particle number ratios. This study aimed at understanding how the presence of microgel particles with different individual elastic moduli affects the overall elasticity of heterogeneous microgel packings. The microgel packing fractions investigated cover the range from the onset of elasticity to very large packing ($\zeta \approx 5$), at which the microgels are strongly deformed and deswollen. This allowed the transition from the mechanics of a particulate suspension to the mechanics of a continuum to be studied. This work reveals that at low packing the shear elasticity of heterogeneous microgel suspensions containing up to 50% of stiff microgel particles is mostly due to the response of the soft, easily deformable microgel particles; in contrast, at high packing, both soft and stiff microgels contribute to the packing elasticity. This is due to the fundamentally different origin of elasticity at different microgel packing: whereas at low packing the elasticity is controlled by soft repulsive interactions between the contact facets of the particles, at high packing the elasticity is governed by rubber-like elasticity that reflects both soft and stiff contributions.

3.6 *Counter-effect of Brownian and elastic forces on the liquid-to-solid transition of microgel suspensions*

F. Di Lorenzo and S. Seiffert, *Soft Matter,* **2015**, *11*, 5235–5245.
DOI: 10.1039/C5SM00881F.

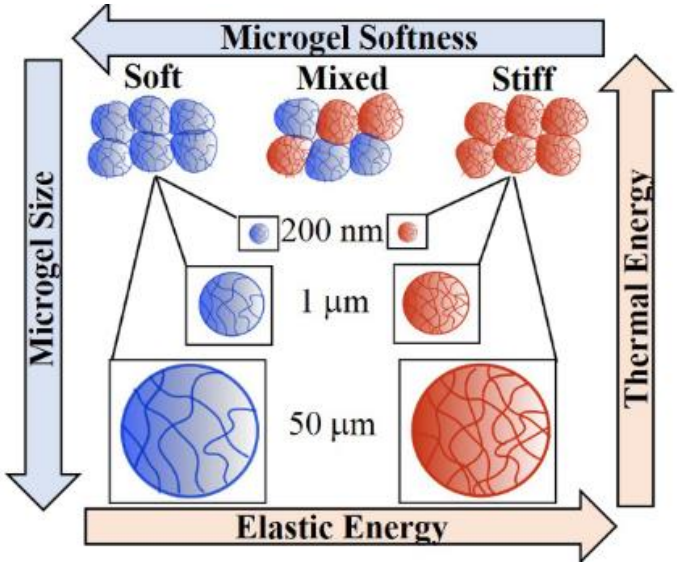

Author contributions:

F. Di Lorenzo**:** Synthesis of microgels, dynamic light scattering, viscosity measurements, osmotic compression, shear rheology measurements and data analysis, project development, preparation of the manuscript.

S. Seiffert: Conception and supervision of the work, correction of the manuscript.

In this work, the transition of suspensions of pNIPAm microgels from liquid-like to solid-like mechanics with increasing microgel packing fraction was investigated by shear rheology, with a focus on the effect of the microgel softness and size on the occurrence of this transition. The softness of the microgels was tuned by varying their crosslinking density, while their size was simultaneously and independently varied from 200 nm, to 1 µm, to 50 µm. The colloidal-scale microgels were synthesized by precipitation polymerization, while the granular-scale microgels were prepared by droplet-templated polymerization in microfluidic devices. This work indicates that a contra-balance between Brownian and elastic forces controls the liquid-to-solid transition of microgel suspensions. As a result, the microgel packing fraction at which this transition occurs depends on both the size and the softness of the microgel particles, such that small and soft microgels undergo this transition at much larger packing fractions than stiff microgels of the same size and than larger microgels with the same softness. This work suggests a systematic strategy to quantitatively predict this transition.

4. Summary and Conclusions

In the first part of this thesis, the effect of network defects and of a spatially inhomogeneous distribution of the crosslinking density on the physical properties of macroscopic polymer gels was investigated. These studies indicate that the mobility of self-diffusing linear flexible polymer chains in heterogeneous polymer networks exhibiting a wide distribution of network strand lengths is independent of the network heterogeneity. This was observed both in the case of diffusing tracer chains that are smaller than the average network strand length and can therefore freely diffuse in the network, and in the case of tracer chains that are larger than the average network strand length and must therefore reptate in a tube-like region defined by the crosslinking junctions. These observations were explained with the hypothesis that the tracer chains diffuse more slowly through densely crosslinked network domains and faster in loosely crosslinked network domains; however, their spatially and temporally averaged diffusion coefficients were found to depend only on the *average* network strand length, and not on the distribution of network strand lengths. These results indicate that when polymer gels prepared by uncontrolled polymerization methods are used as filtering membranes,[6–10] or for the encapsulation and the release of drugs, the gel permeability is not significantly affected by nanostructural heterogeneity.[11–16]

Other promising applications of synthetic polymer gels are the mimic of soft biological tissues such as muscles and tendons,[20] or the use as superabsorber materials:[5] in both these applications, the achievement of a good control of the gel elasticity is crucial. In this thesis, the elasticity of swollen polymer gels was studied with respect to their more homogeneous or more inhomogeneous distributions of crosslinking density. The elastic moduli of these gels was measured both on a macroscopic length scale by shear rheology and on a microscopic length scale by atomic force microscopy. These studies revealed that in gels with homogeneously distributed crosslinking density, the elastic modulus is independent of the length scale of observation. If, in contrast, the crosslinking density exhibits strong spatial concentration fluctuations, the measured elastic modulus decreases when the experimental length scale becomes larger than the length scale of structural inhomogeneities. These results were explained with the concept of non-affine deformation of the different nanoscopic gel domains, with the densely crosslinked domains embedded within an easily deformable, less crosslinked background that mostly contributes to the gel elasticity. These findings suggest that when polymeric gels are used as

superabsorbent materials or to mimic biological tissues, it should be considered that their mechanical properties vary with the size of the commonly present polymer network inhomogeneities, and with the length scale on which these properties are relevant for a given application.

The nanostructure of macroscopic polymer gels exhibiting inhomogeneous crosslinking density was also modelled in this work by densely packed microgel suspensions containing a major fraction of soft microgels mixed with a minor fraction of stiff microgels. These studies demonstrate that in heterogeneous microgel packings with fixed particle packing geometry, both soft and stiff microgels contribute to the overall elastic modulus, which linearly increases with the density of crosslinking junctions, as appraised by the theory of rubber elasticity.

In the second part of this thesis, the transition of suspensions of microgel particles from liquid-like to solid-like mechanics with increasing microgel packing fraction was investigated by shear rheology, focusing on the effect of the particle softness and size on this transition. These studies revealed that the occurrence of this transition depends on the ratio between the thermal energy, k_BT, and the elastic energy, ε, of its constituent microgels, in agreement with recent simulations.[204] The experiments of this work showed that suspensions of pNIPAm microgels with sizes of ≈ 1 μm and of ≈ 50 μm undergo a jamming transition if they are packed above the microgel packing fraction of $\zeta \approx 0.64$, independently of the particle softness. This occurs because in these suspensions the thermal energy of the microgels is much smaller than their elastic energy ($k_BT/\varepsilon \leq 10^{-7}$). By contrast, it was found that suspensions of ≈ 200 nm-sized pNIPAm microgels undergo a glass-analogous liquid-to-solid transition, and that the microgel packing fraction at which this transition occurs increases from $\zeta \approx 0.58$ to $\zeta > 9$ with increasing microgel softness. These findings were explained by the larger ratio between the thermal and the elastic energy of their constituent microgels ($k_BT/\varepsilon \approx 10^{-5}$–$10^{-4}$). This general picture suggests a strategy to quantitatively predict the shear elasticity and the occurrence of the liquid-to-solid transition of suspensions of particles of known size and softness.

In addition, the shear elasticity of heterogeneous microgel suspensions containing soft and stiff microgels of the same size mixed in different particle number ratios was also investigated. These studies indicate that in jammed packings of ≈ 1 μm-sized and ≈ 50 μm-sized microgels containing a major fraction of soft microgels mixed with a minor fraction of stiff microgels, it is mostly the soft and better deformable microgels that carry the burden of elastic energy storage. In these heterogeneous microgel packings, the stiff microgels were found to contribute to the elasticity only if these microgels are present in major amounts and are therefore percolated. By contrast, in heterogeneous packings of soft and stiff ≈ 200 nm-sized microgels

approaching the colloidal glass transition, both types of microgels were found to contribute to elasticity, even if the stiff microgels are present in a minor amount.

The elasticity of microgel suspensions was also probed in a range of packing fractions at which the microgels are so densely packed that the particle packing geometry becomes fixed, resulting in a crossover from particulate mechanics to continuum mechanics. These studies revealed that in suspensions of stiff microgels this crossover occurs at a packing fraction of $\zeta \approx 1-1.6$ and is independent of the size of the microgels. By contrast, in suspensions of soft microgels, the microgel packing fraction at which this crossover occurs was found to increase strongly with decreasing microgel size from $\zeta \approx 1.4$ to $\zeta >> 9$. These observations indicate that in dense packings of small and soft microgels, the contribution of Brownian motion to the dynamics is more relevant than in packings of stiff microgels, whose geometry is fixed at packing fractions close to space-filling.

5. Zusammenfassung und Fazit

Im ersten Teil dieser Arbeit wurde der Effekt von Netzwerkdefekten und von einer räumlich inhomogenen Verteilung der Vernetzungsdichte auf die physikalischen Eigenschaften makroskopischer Polymergele untersucht. Diese Studien zeigten, dass die Mobilität von selbst-diffundierenden linearen flexiblen Polymerketten in heterogenen Polymernetzwerken, die eine breite Verteilung an Netzwerkmaschenweiten aufweisen, unabhängig von dieser Heterogenität ist. Dies wurde im Fall von diffundierenden Polymerketten beobachtet, die kleiner als die durchschnittliche Maschenweite des Netzwerkes sind, und die daher im Netzwerk vermutlich frei diffundieren können. Außerdem wurden dieselben Ergebnisse im Fall von diffundierenden Polymerketten erzielt, die ausgedehnter als die durchschnittliche Maschenweite des Netzwerkes sind, und deren Mobilität durch die Vernetzungpunkte eingeschränkt ist. Solche Polymerketten können aus diesem Grund nur innerhalb einer rohrförmigen Region des Netzwerkes, die von den Vernetzungpunkten bestimmt wird, mit einer Reptilien-ähnlichen Bewegung diffundieren [*Englisch*, „reptate“]. Die Ergebnisse dieser Studien wurden mit der Hypothese erklärt, dass die Mobilität der diffundierenden Polymerketten in eng vernetzen Netzwerkdomänen niedriger ist als ihre Mobilität in lose vernetzten Netzwerkdomänen. Allerdings hängt ihr über Zeit und Raum gemittelter Diffusionskoeffizient nur von der durchschnittlichen Maschenweite des Netzwerkes ab und nicht von der Verteilung der Maschenweiten. Diese Ergebnisse zeigen, dass nanostrukturelle Heterogenenität keinen bedeutenden Effekten auf die Permeabilität von heterogenen Polymergelen hat, die mit unkontrollierten Polymerisationsmethoden hergestellt wurden und als Filtermembranen[6–10] oder für die Verkapselung und die Freisetzung von Medikamenten[11–16] benutzt werden.

Andere vielversprechende Anwendungsgebiete synthetischer Polymergele sind die Nachahmung weicher biologischer Gewebe wie Muskeln und Sehnen[20] und der Gebrauch als Superabsorbermaterialen.[5] In beiden dieser Anwendungen ist eine gute Kontrolle der Elastizität der Polymergele erforderlich. Aus diesem Grund wurde in dieser Arbeit die Elastizität gequollener Polymergele mit Bezug auf die homogene oder inhomogene Verteilung ihrer Vernetzungsdichte untersucht. Die Elastizitätsmoduli dieser Gele wurden auf einer makroskopischen Längenskala mittels Scherrheologie und auf einer mikroskopischen Längenskala mittels Rasterkraftmikroskopie gemessen. Diese Untersuchungen zeigten, dass der Elastizitätsmodul von Gelen, die eine größtenteils homogen verteilte Vernetzungsdichte aufweisen, unabhängig von der experimentellen Längenskala ist. Im Gegensatz dazu nimmt der

Elastizitätsmodul von Gelen, die starke Fluktuationen in der Vernetzungsdichte aufweisen, zu, wenn die experimentelle Längenskala größer als die Längenskala der strukturellen Inhomogenitäten wird. Diese Ergebnisse wurden durch das Konzept von nicht-affiner Deformation der unterschiedlichen Netzwerkdomänen erklärt, wobei die eng vernetzten Domänen in einem lose vernetzten, besser deformierbaren Untergrund eingebettet sind, der größtenteils zum Elastizitätsmodul des Gels beiträgt. Diese Resultate deuten darauf hin, dass bei der Verwendung von Polymergelen als Superabsorbermaterialen oder in der Nachahmung biologischer Gewebe berücksichtig werden sollte, dass die mechanischen Eigenschaften dieser Gele mit der Längenskala ihrer strukturellen Inhomogenität variieren, verglichen mit der Längenskala auf der die mechanischen Eigenschaften für eine bestimmte Anwendung relevant sind.

Die Nanosktruktur von makroskopischen Polymergelen mit inhomogener Vernetzungdichte wurde ebenfalls mit Hilfe von dichtgepackten heterogenen Mikrogelsuspensionen imitiert, die zu einem höheren Anteil aus weichen Mikrogelen und zu einem niedrigeren Anteil aus steifen Mikrogelen bestanden. Die darauffolgenden Untersuchungen zeigten, dass in gepackten heterogenen Mikrogelsuspensionen mit fixierter Packungsgeometrie sowohl weiche als auch steife Mikrogele zur Gesamtelastizität beitragen. Der Elastizitätsmodul dieser Mikrogelsuspensionen nimmt linear mit zunehmender Vernetzungsdichte zu, in Übereinstimmung mit der Theorie der Gummielastizität für makroskopische Polymergele.

Im zweiten Teil dieser Arbeit wurde der Übergang einer Mikrogelsuspension von einer Flüssigkeit zu einem Feststoff mit zunehmender Mikrogelkonzentration mittels Scherrheologie untersucht. Im Fokus dieser Untersuchungen stand insbesondere der Effekt von der Weichheit und von der Größe der Mikrogele auf diesen Übergang. Aus diesen Studien ergab sich, dass das Auftreten dieses Übergangs vom Verhältnis der thermischen Energie, k_BT, und der elastischen Energie der Mikrogele, ε, abhängt, in Übereinstimmung mit einer vor kurzem veröffentlichten Simulationsstudie.[204] Die Experimente dieser Arbeit zeigten, dass Suspensionen von ≈ 1 μm und ≈ 50 μm großen pNIPAm Mikrogelpartikeln einen Übergang von einem flüssigen zu einem dichtgepackten [*English*, „jammed“] Zustand eingehen. Dieser Übergang findet in Suspensionen mit einer Mikrogelpackungsdichte von $\zeta \approx 0.64$ statt und ist unabhängig von der Weichheit der Mikrogele. Diese Beobachtung wurde dadurch erklärt, dass die thermische Energie der Mikrogele viel kleiner als ihre elastische Energie ist ($k_BT/\varepsilon \leq 10^{-7}$). Im Gegensatz dazu zeigen Suspensionen von 200 nm großen Mikrogelen einen Übergang von

flüssig zu fest, der dem Glasübergang ähnelt. Außerdem nimmt die Mikrogelpackungsdichte, bei der dieser Übergang auftritt, mit zunehmender Mikrogelweichheit von $\zeta \approx 0.58$ auf $\zeta > 9$ zu. Dieses Resultat wurde durch das grössere Verhältnis von thermischer Energie und elastischer Energie der Mikrogele begründet ($k_B T/\varepsilon \approx 10^{-4}–10^{-5}$). Dieses generelle Bild deutet auf eine Strategie hin, um die Scherelastizität und das Auftreten des flüssig-fest-Übergangs von Suspensionen mit bekannter Partikelgröße und -weichheit quantitativ voherzusagen.

Weiterhin wurde die Elastizität heterogener Mikrogelsuspensionen, die unterschiedliche Mischungsanteile weicher und steifer Mikrogele enthielten, untersucht. Aus diesen Experimenten ergab sich, dass in „jammed“ Mikrogelsuspensionen von ≈ 1 µm und ≈ 50 µm großen Mikrogelpartikeln, die einen höheren Anteil an weichen Mikrogelen und einen niedrigeren Anteil an steifen Mikrogelen enthalten, fast ausschließlich die weichen und besser deformierbaren Mikrogele für die Speicherung elastischer Energie verantwortlich sind. Die steifen Mikrogele tragen zur Elastizität solcher heterogener Mikrogelpackungen nur bei, wenn diese Mikrogele in überwiegenden Anteilen vorkommen und daher perkoliert sind. Im Gegensatz dazu tragen in heterogenen Packungen von weichen und steifen ≈ 200 nm großen Mikrogelpartikeln, die einen Glasübergang zeigen, beide Arten von Mikrogelen zur Elastizität bei, selbst wenn die steifen Mikrogele zu einem geringen Anteil vorliegen.

Die Elastizität von Mikrogelsuspensionen wurde auch bei Mikrogelpackungsdichten untersucht, bei denen die Mikrogelpartikel so dicht gepackt sind, dass die Packungsgeometrie fixiert wird: Dadurch weisen diese Suspensionen einen Übergang von der Mechanik eines Partikelensembles zur Mechanik eines kontinuierlichen Materials auf. Aus diesen Studien ergab sich, dass dieser Übergang in gepackten Suspensionen steifer Mikrogele bei einer Mikrogelpackungsdichte $\zeta \approx 1−1.6$ auftritt, und dass diese Packungsdichte unabhängig von der Größe der Mikrogele ist. Im Gegensatz dazu nimmt in Suspensionen weicher Mikrogele die Packungsdichte dieses Übergangs mit abnehmender Mikrogelgröße von $\zeta \approx 1.4$ auf $\zeta >> 9$ zu. Diese Beobachtungen deuten darauf hin, dass in raumfüllenden Suspensionen von kleinen und weichen Mikrogelpartikeln der Beitrag Brownscher Bewegung zur Dynamik relevanter ist als in Packungen steifer Mikrogele, bei denen die Packungsgeometrie im raumfüllenden Packungen fixiert ist.

6 References

[1] K. Almdal, J. Dyre, S. Hvidt and O. Kramer, *Polym. Gels Netw*., **1993**, *1*, 5−17.

[2] T. Tanaka, in *Encyclopedia of Polymer Science and Engineering*, vol. 7, ed. A. Klingsberg & R. Piccininni, John Wiley & Sons, New York, 1987.

[3] A. D. Jenkins, P. Kratochvìl, R. F. T. Stepto and U. W. Suter, *Pure Appl. Chem.*, **1996**, *68*, 2287−2311.

[4] W. Funke, O. Okay and B. Joos-Müller, *Adv. Polym. Sci*., **1998**, *136*, 139−234.

[5] F. L. Buchholz and T. Graham in *Modern superabsorbent polymer technology*, Wiley-VCH, New York, 1998.

[6] H. Kanazawa, T. Sunamoto, E. Ayano, Y. Matsushima, A. Kikuchi and T. Okano, *Anal. Sci.,* **2002**, *18*, 45–48.

[7] E. A. S. Doherty, C.-W. Kan, B. M. Paegel, S. H. I. Yeung, S. Cao, R. A. Mathies and A. E. Barron, *Anal. Chem.*, **2004**, *76*, 5249–5256.

[8] O. Wang, S. Samitsu and I. Ichinose, *Adv. Mater.*, **2011**, *23*, 2004–2008.

[9] R. F. Childs*,* A. M. Mika*,* A. K. Pandey*,* C. McCrory*,* S. Mouton and J. M. Dickson*, Sep. Purif. Technol.,* **2001***, 22–23,* 507−517.

[10] B. Mizrahi, S. Irusta, M. McKenna, C. Stefanescu, L. Yedidsion, M. Myint, R. Langer and D. S. Kohane, *Adv. Mater*. **2011**, *23*, H258−262.

[11] J. Lia, N. Wanga and X. S. Wua, *J. Controlled Release*, **1998**, *56*, 117−126.

[12] K. S Soppimatha, T. M Aminabhavia, A. R Kulkarnia and W. E Rudzinskib, *J. Controlled Release*, **2001**, *70*, 1−20.

[13] S. V. Vinogradov, T. K. Bronich and A. V. Kabanov, *Adv. Drug Delivery Rev.,* **2002**, *54*, 135–147.

[14] T. R. Hoare and D. S. Kohane, *Polymer*, **2008**, *49*, 1993−2007.

[15] D. Sivakumaran*,* D. Maitland and T. Hoare*, Biomacromolecules*, **2011***, 12,* 4112–4120*.*

[16] A. V. Kabanov and S. V. Vinogradov, *Angew. Chem. Int. Ed*., **2009**; *48,* 5418–5429.

[17] Y. Lu, S. Proch, M. Schrinner, M. Drechsler, R. Kempe and M. Ballauff, *J. Mater. Chem*., **2009**, *19*, 3955−3961.

[18] N. Welsch, M. Ballauff and Y. Lu, *Adv. Polym. Sci.*, **2011**, *234*, 129–163.

[19] S. Wu, J. Dzubiella, J. Kaiser, M. Drechsler, X. Guo, M. Ballauff and Y. Lu, *Angew. Chem. Int. Ed*., **2012**, *51*, 2229–2233.

[20] J. Ping Gong, *Science*, **2014**, *344,* 161–162.

[21] O. Wichterle and D. Lim, *Nature*, **1960**, *185*, 117−118.

[22] D. Braun, *Int. J. Polym. Sci*., **2009**, *2009*, 1−10.

[23] J. C. Hernández-Ortiz and E. Vivaldo-Lima, in *Handbook of Polymer Synthesis, Characterization, and Processing*, ed. E. Saldivar-Guerra and E. Vivaldo-Lima, John Wiley and Sons, Hoboken, New Jersey, 2013.

[24] M. Akiba and A. S. Hashim, *Prog. Polym. Sci.*, **1997**, *22*, 475−521.

[25] H. G. Schild, *Prog. Polym. Sci.*, **1998**, *23*, 1019–1149.

[26] T. Sakai, T. Matsunaga, Y. Yamamoto, C. Ito, R. Yoshida, S. Suzuki, N. Sasaki, M. Shibayama and U.-I. Chung, *Macromolecules*, **2008**, *41*, 5379–5384.

[27] A. Elaïssari in *Handbook of Surface and Colloid Chemistry*, ed. K. S. Birdi, CRC Press, Roca Baton, Florida, 2009.

[28] K. Landfester, M. Willert and M. Antonietti, *Macromolecules*, **2000**, *33*, 2370–2376.

[29] R. K. Shah, J. W. Kim, J. J. Agresti, D. A. Weitz and L. Y. Chu, *Soft Matter*, **2008**, *4*, 2303–2309.

[30] R. K. Shah, H. C. Shum, A. C. Rowat, D. Lee, J. J. Agresti, A. S. Utada, L. Chu, J. Kim, A. Fernandez-Nieves, C. J. Martinez and D. A. Weitz, *Mater. Today*, **2008**, *11*, 18–27.

[31] S. Seiffert, *ChemPhysChem,* **2013**, *14*, 295–304.

[32] A. S. Utada, E. Lorenceau, D. R. Link, P. D. Kaplan, H. A. Stone and D. A. Weitz, *Science*, **2005**, *308*, 537–541.

[33] Y. Xia and G. M. Whitesides, *Angew. Chem. Int. Ed.,* **1998**, *37*, 550–575.

[34] J.-W. Kim, A. S. Utada, A. Fernández-Nieves, Z. Hu and D. A. Weitz, *Angew. Chem.,* **2007**, *119*, 1851–1854.

[35] S. Seiffert and D. A. Weitz, *Soft Matter,* **2010**, *6*, 3184–3190.

[36] S. Seiffert, J. Thiele, A. R. Abate and D. A. Weitz, *J. Am. Chem. Soc.,* **2010**, *132*, 6606–6609.

[37] S. Seiffert, M. B. Romanowsky and D. A. Weitz, *Langmuir,* **2010**, *26*, 14842–14847.

[38] M. Heskins and J. E. Guillet, *J. Macromolec. Sci. Chem.,* **1969,** *2*, 1441−1455.

[39] H.G. Schild, *Prog. Polym. Sci.,* **1992**, *17*, 163−249.

[40] S. Hirotsu, *J. Phys. Soc. Jpn*., **1987**, *56*, 233−242.

[41] Y. Li and T. Tanaka, *Annu. Rev. Mater. Sci.*, **1992**, *22*, 243–277.

[42] M. Shibayama and T. Tanaka, *Adv. Polym. Sci*., **1993**, *109*, 1–62.

[43] H. Ringsdorf, J. Venzmer and F. M. Winnik, *Macromolecules,* **1991***, 24*, 1678–1686.

[44] A. Pollak, H. Blumenfeld, M. Wax, R. L. Baughn and G. M. Whitesides, *J. Am. Chem. Soc.,* **1980***, 102*, 6324–6236.

[45] F. M. Winnik, *Macromolecules,* **1990***, 23,* 233–242.

[46] T. Rossow, S. Hackelbusch, P. Van Assenbergh and S. Seiffert, *Polymer Chem.,* **2013**, *4*, 2515–2527.

[47] N. Nagaoka, A. Safranj, M. Yoshida, J. H. Omichi, H. Kubota and R. Katakai, *Macromolecules*, **1993**, *26*, 7386−7388.

[48] S. Seiffert and W. Oppermann, *Macromol. Chem. Phys*., **2007**, *208*, 1744–1752.

[49] S. Seiffert, K. Saalwächter and W. Oppermann, *Polymer,* **2007**, *48*, 5599–5611.

[50] X. Yu, C. Corten, H. Goerner, T. Wolff and D. Kuckling, *J. Photochem. Photobiol., A*, **2008**, *198*, 34–44.

[51] R. H. Pelton and P. Chibante, *Colloids Surf*., **1986**, *20*, 247–256.

[52] R. Pelton, *Adv. Colloid Interface*, **2000**, *85*, 1−33.

[53] W. McPhee, K. C. Tam and R. Pelton, *J. Colloid Interface Sci*., **1993**, *156*, 24–30.

[54] X. Wu, R. H. Pelton, A. E. Hamielec, D. R. Woods and W. McPhee, *Colloid Polym. Sci*., **1994**, *272*, 467−477.

[55] H. Shimizu, R. Wada and M. Okabe, *Polym. J*., **2009**, *41*, 771–777.

[56] K. Kratz, T. Hellweg and W. Eimer, *Colloids Surf. A*, **2000**, *170*, 137–149.

[57] M. J. García-Salinas, M. S. Romero-Cano and F. J. de las Nieves, *J. Colloid Interf. Sci*., **2002**, *248*, 54–61.

[58] T. López-León, J. L. Ortega-Vinuesa, D. Bastos-González and A. Elaïssari, *J. Phys. Chem. B*, **2006**, *110*, 4629–4636.

[59] H. Nur, V. T. Pinkrah, J. C. Mitchell, L. S. Benée and M. J. Snowden, *Adv. Colloid Interface Sci*., **2010**, *158*, 15–20.

[60] S. Nöjd, P. S. Mohanty, P. Bagheri, A. Yethiraj and P. Schurtenberger, *Soft Matter*, **2013**, *9*, 9199–9207.

[61] W. H. Blackburn and L. A. Lyon, *Colloid. Polym. Sci*., **2008**, *286*, 563–569.

[62] S. Zhou and B. Chu, *J. Phys. Chem. B*, **1998**, *102*, 1364–1371.

[63] N. J. Flint, S. Gardebrecht and L. Swanson, *J. Fluoresc*., **1998**, *8*, 343–353.

[64] J. D. Debord and L. A. Lyon, *Langmuir*, **2003**, *19*, 7662–7664.

[65] M. Keerl and W. Richtering, *Colloid Polym. Sci*., **2007**, *285*, 471–474.

[66] P. Menut, S. Seiffert, J. Sprakel and D. A. Weitz, *Soft Matter,* **2012**, *8*, 156–164.

[67] S. Seiffert, *Macromol. Rapid Commun.,* **2012**, *33*, 1135–1142.

[68] A. Habicht, W. Schmolke, F. Lange, K. Saalwächter and S. Seiffert, *Macromol. Chem. Phys.,* **2014**, *215*, 1116–1133.

[69] K. Dušek and W. Prins, *Adv. Polym. Sci.,* **1969**, *6*, 1–102.

[70] N. Weiss, T. T. Van Vliet and A. Silberberg, *J. Polym. Sci., Polym. Phys. Ed.*, **1979**, *17*, 2229–2240.

[71] M. Shibayama, *Macromol. Chem. Phys.*, **1998**, *199*, 1–30.

[72] N. Weiss, T. T. Van Vliet and A. Silberberg, *J. Polym. Sci., Polym. Phys. Ed*., **1981**, *19*, 1505–1512.

[73] F. Di Lorenzo and S. Seiffert, *Polymer Chem.*, **2015**, DOI: 10.1039/C4PY01677G.

[74] J. Bastide and L. Leibler, *Macromolecules,* **1988**, *21*, 2649–2651.

[75] E. Mendes Jr, P. Lindner, M. Buzier, F. Boué and J. Bastide, *Phys. Rev. Lett*., **1991**, *66*, 1595–1598.

[76] W. Chassé, S. Schlögl, G. Riess and K. Saalwächter, *Soft Matter*, **2013**, *9*, 6943–6954.

[77] M. Shibayama, *Polym. J*., **2011**, *43*, 18–34.

[78] H. Tobita and A. E. Hamielec, *Polymer*, **1990**, *31*, 1546–1552.

[79] H. Tobita, *Polymer*, **1992**, *33*, 3647–3657.

[80] O. Okay, H. J. Nagash and I. Capek, *Polymer,* **1995**, *36*, 2413–2419.

[81] M. Y. Kizilay and O. Okay, *Polymer*, **2003**, *44*, 5239–5250.

[82] B. Lindemann, U. P. Schröder and W. Oppermann, *Macromolecules,* **1997**, *30,* 4073–4077.

[83] G. Patras, G. G. Qiao and D. H. Solomon, *Macromolecules*, **2001**, *34*, 6396–6401.

[84] J. Nie, B. Du and W. Oppermann, *Macromolecules,* **2004**, *37*, 6558–6564.

[85] N. Orakdogen and O. Okay, *Polym. Bull.,* **2006**, *57*, 631–641.

[86] S. Takata, T. Norisuye and M. Shibayama, *Macromolecules,* **1999**, *32*, 3989–3993.

[87] Y. Hirokawa, H. Jinnai, Y. Nishikawa, T. Okamoto and T. Hashimoto, *Macromolecules,* **1999**, *32*, 7093–7099.

[88] K. Saalwächter*, Progr. NMR Spectrosc.,* **2007***, 51*, 1–35.

[89] K. Saalwächter, *J. Am. Chem. Soc*., **2003**, *125*, 14684–14685.

[90] J. L. Valentín, P. Posadas, A. Fernandez-Torres, M. A. Malmierca, L. Gonzalez, W. Chassé and K. Saalwächter, *Macromolecules,* **2010**, *43*, 4210–4222.

[91] W. Chassé, M. Lang, J. Sommer and K. Saalwächter, *Macromolecules,* **2012**, *45*, 899−912.

[92] J. Höpfner, G. Guthausen, K. Saalwächter and M. Wilhelm, *Macromolecules,* **2014**, *47*, 4251−4265.

[93] A. Suzuki, M. Yamazaki and Y. Kobiki, *J. Chem. Phys*., **1996**, *104*, 1751–1757.

[94] D. R. Kioussis and P. Kofinas, *Polymer*, **2005**, *46*, 10167–10172.

[95] I. M. Barszczewska-Rybarek and M. Krasowska, *Dent. Mater.*, **2012**, *28*, 695–702.

[96] H. Aoki, S. Tanaka, S. Ito and M. Yamamoto, *Macromolecules,* **2000**, *33*, 9650–9656.

[97] F. B. Madsen, A. E. Daugaard, C. Fleury, S. Hvilsted and A. L. Skov, *RSC Adv.*, **2014**, *4*, 6939–6945.

[98] G. E. Mitchell, L. R. Wilson, M. T. Dineen, S. G. Urquhart, F. Hayes, E. G. Rightor, A. P. Hitchcock and H. Ade, *Macromolecules,* **2002**, *35*, 1336–1341.

[99] T. Hsu and C. Cohen, *Polymer*, **1984**, *25*, 1419–1423.

[100] J. Shan, J. Chen, Z. Liu and M. Zhang, *Polym. J.*, **1996**, *28*, 886–892.

[101] G. Patras, G. G. Qiao and D. H. Solomon, *Macromolecules*, **2001**, *34*, 6396–6401.

[102] M.Y. Kizilay and O. Okay, *Polymer,* **2004**, *45*, 2567–2576.

[103] M. Y. Kizilay and O. Okay, *Macromolecules,* **2003**, *36*, 6856–6862.

[104] S. Takata, T. Norisuye and M. Shibayama, *Macromolecules,* **1999**, *32*, 3989–3993.

[105] Y. Hirokawa, H. Jinnai, Y. Nishikawa, T. Okamoto and T. Hashimoto, *Macromolecules,* **1999**, *32*, 7093–7099.

[106] M. Shibayama, F. Ikkai, Y. Shiwa and Y. Rabin, *J. Chem. Phys.,* **1997**, *107*, 5227–5235.

[107] Liu and W. Oppermann, *Macromolecules*, **2006,** *39*, 4159–4167.

[108] N. Gundogan, O. Okay and W. Oppermann, *Macromol. Chem. Phys*., **2004**, *205*, 814–823.

[109] S. Mallam, F. Horkay, A. M. Hecht and E. Geissler, *Macromolecules,* **1989**, *22*, 3356–3361.

[110] G. R. Deen, T. Alsted, W. Richtering and J. S. Pedersen, *Phys. Chem. Chem. Phys*., **2011**, *13*, 3108–3114.

[111] M. Shibayama, K. Kawakubo, F. Ikkai and M. Imai, *Macromolecules*, **1998**, *31*, 2586–2592.

[112] T. Norisuye, N. Masui, Y. Kida, M. Shibayama, D. Ikuta, E. Kokufuta, S. Ito and S. Panyukov, *Polymer,* **2002**, *43*, 5289–5297.

[113] S. Takata, T. Norisuye and M. Shibayama, *Macromolecules*, **2002**, *35*, 4779–4784.

[114] T. Norisuye, Y. Kida, N. Masui, Q. Tran-Cong-Miyata, Y. Maekawa, M. Yoshida and M. Shibayama, *Macromolecules,* **2003**, *36*, 6202–6212.

[115] S. Koizumia, M. Monkenbusch, D. Richter, D. Schwahn and B. Farago, *J. Chem. Phys*., **2004**, *121*, 12721–12731.

[116] M. Shibayama, *Bull. Chem. Soc. Jpn*., **2006**, *79*, 1799–1819.

[117] P. Debye and A. M. Bueche, *J. Appl. Phys.,* **1949**, *20*, 518–525.

[118] P. Debye, H. R. Anderson and H. Brumberger, *J. Appl. Phys.,* **1957**, *28*, 679–683.

[119] F. Bueche, *J. Colloid Interface Sci*., **1970**, *33*, 61–66.

[120] V. K .Soni and R. S. Stein, *Macromolecules*, **1990**, *23*, 5257−5265.

[121] H. Furukawa, K. Horie, R. Nozaki and M. Okada, *Phys. Rev. E,* **2003**, *68***,** 031406–14.

[122] T. Norisuye, Q. Tran-Cong-Miyata and M. Shibayama, *Macromolecules,* **2004**, *37*, 2944–2953.

[123] F. J. Giessibl, *Rev. Mod. Phys*., **2003**, *75*, 949–983.

[124] N. Jalili and K. Laxminarayana, *Mechatronics*, **2004**, *14*, 907–945.

[125] R. A. Marklein and J. A. Burdick, *Soft Matter*, **2010**, *6*, 136–143.

[126] M. V. Flores-Merino, S. Chirasatitsin, C. LoPresti, G. C. Reilly, G. Battaglia and A. J. Engler, *Soft Matter*, **2010**, *6*, 4466–4470.

[127] Z. Drira and V. K. Yadavalli, *J. Mech. Behav. Biomed*., **2013**, *18*, 20–28.

[128] K. H. Meyer, G. von Susich and E. Valkó, *Kolloid Z*., **1932**, *59*, 208–216.

[129] P. J. Flory in *Principles of Polymer Chemistry*, Cornell University Press, New York, 1953.

[130] P. J. Flory, *Polym. J*., **1985**, *17*, 1–12.

[131] E. Guth and H. H. James, *Ind. Eng. Chem*., **1941**, *33*, 624–629.

[132] P. J. Flory and J. Jr. Rehner, *J. Chem. Phys*., **1943**, *11*, 512–520.

[133] H. M. James, *J. Chem. Phys*., **1947**, *15*, 651–668.

[134] H. M. James and E. Guth, *J. Chem. Phys.,* **1947***, 15*, 669–683.

[135] W. Kuhn and F. Grün*, J. Polymer Sci*., **1946***, 1,* 183–199.

[136] L. R. G. Treloar, *Trans. Faraday Soc.,* **1944**, *40*, 59–70.

[137] P. J. Flory, *Chem. Revs*., **1944**, *35*, 51–75.

[138] P. J. Flory, N. Rabjohn and M. C. Shaffer, *J. Polym. Sci*., **1949**, *4*, 225–245.

[139] J. Scanlan, *J. Polym. Sci*., **1960**, *43*, 501–508.

[140] L. C. Case, *J. Polym. Sci*., **1960**, *45*, 39–404.

[141] H. M. James and E. Guth, *J. Chem. Phys*., **1943**, *11,* 455–481.

[142] L. R. G. Treolar, *Rep. Prog. Phys.,* **1973**, *36*, 755–826.

[143] P. J. Flory, *Macromolecules,* **1982**, *15*, 99–100.

[144] A. L. Andrady, M. A. Llorente and J. E. Mark, *J. Chem. Phys*., **1980**, *72*, 2282–2290.

[145] A. L. Andrady, M. A. Llorente and J. E. Mark, *J. Chem. Phys*., **1980**, *73*, 1439–1445.

[146] Z.-M. Zhang and J. E. Mark, *J. Polymer Sci. Pol. Phys*., **1982**, *20*, 473–480.

[147] J. E. Mark and M.-Y. Tang, *J. Polymer Sci. Pol. Phys*., **1984**, *22*, 1849–1855.

[148] M. Tang and J. E. Mark, *Macromolecules,* **1984**, *17*, 2616–2619

[149] S.-J. Pan and J.E. Mark, *Polym. Bull.,* **1982**, *7*, 553–559.

[150] B. D. Viers and J. E. Mark, *J. Macromol. Sci.,* **2007**, *44*, 131–138.

[151] J. R. Falender, *G.* S. Y. Yeh and J. E. Mark, *J. Am. Chem. Soc*., **1979**, *101*, 7353–7356.

[152] R. Liu and W. Oppermann, *Macromolecules*, **2009**, *42*, 9195–9198.

[153] S. Grube and W. Oppermann, *Macromolecules,* **2013**, *46*, 1948−1955.

[154] A. Einstein, *AdP*, **1905**, *17*, 549–560.

[155] A. Einstein, *AdP*, **1906**, *19,* 371–381.

[156] P. E. Rouse Jr., *J. Chem. Phys*., **1953**, *21*, 1272–1280.

[157] P.-G. De Gennes, *J. Chem. Phys*., **1971**, *55*, 572–579.

[158] P. -G. De Gennes, *Macromolecules*, **1976**, *9*, 587–593.

[159] P. -G. De Gennes, *Macromolecules*, **1976**, *9*, 594–59.

[160] J. Klein*, Nature,* **1978***, 271,* 143–145.

[161] P.-G. de Gennes in *Scaling Concepts in Polymer Physics*, Cornell University Press, Ithaca, 1979.

[162] P. -G. de Gennes and L. Leger, *Ann. Rev. Phys. Chem*., **1982**. *33*, 49–61.

[163] T. McLeish, *Nature Materials,* **2008***, 7*, 933–935.

[164] E. Arvanitidou and D. Hoagland, *Phys. Rev. Lett*., **1991**, *67*, 1464–1466.

[165] C. R. Calladine, C. M. Collis, H. R. Drew and M. R. Mott, *J. Mol. Biol*., **1991**, *221*, 981–984.

[166] M. Muthukumar and A. Baumgärtner, *Macromolecules,* **1989**, *22*, 1937–1941.

[167] M. Muthukumar and A. Baumgärtner, *Macromolecules,* **1989**, *22,* 1941–1946.

[168] D. A. Hoagland and M. Muthukumar, *Macromolecules,* **1992***, 25,* 6696–6698.

[169] B. H. Zimm and O. Lumpkin, *Macromolecules,* **1993**, *26*, 226–234.

[170] D. Cule and T. Hwa, *Phys. Rev. Lett*., **1998**, *80*, 3145–3148.

[171] S. Pajević, R. Bansil and Č. Koňák, *Macromolecules,* **1993**, *26*, 305–312.

[172] M. Susoff and W. Oppermann, *Macromolecules,* **2010**, *43*, 9100–9107.

[173] S. Seiffert and W. Oppermann, *Polymer,* **2008**, *49*, 4115–4126.

[174] S. Seiffert and W. Oppermann, *J. Microsc,* **2005**, *220*, 20–30.

[175] G. I. Hauser, S. Seiffert and W. Oppermann, *J. Microsc.,* **2008**, *230*, 353–362.

[176] S. Seiffert, *G.I.T., Imaging&Microscopy,* **2007**, *4/2007*, 48–50.

[177] G. L. Hunter and E. R. Weeks, *Rep. Prog. Phys*., **2012**, *75*, 066501.

[178] B. J. Alder and T. E. Wainwright, *J. Chem. Phys.,* **1957**, *27*, 1208–1209.

[179] W. W. Wood and J. D. Jacobson, *J. Chem. Phys*., **1957**, *27*, 1207–1208.

[180] D. Weitz in *Glasses and Grains,* ed. B. Duplantier, T. C. Halsey, V. Rivasseau, 61, Springer, 2011.

[181] G. D. Scott and D. M. Kilgour, *Brit. J. Appl. Phys. (J. Phys. D)*, **1969**, *2*, 863–866.

[182] D. Quemada and C. Berli, *Adv. Colloid Interface Sci*., **2002**, *98*, 51–85.

[183] P. N. Pusey and W. van Megen, *Nature*, **1986**, *320*, 340–342.

[184] P. N. Pusey and W. van Megen, *Phys. Rev. Lett*., **1987**, *59*, 2083–2086.

[185] S. E. Paulin and B. J. Ackerson, *Phys. Rev. Lett*., **1990**, *64*, 2663–2666.

[186] W. Van Megen, P. N. Pusey and P. Bartlett, *Phase Transit*., **1990**, *21*, 207–227.

[187] E. R.Weeks and D. A.Weitz, *Chemical Physics*, **2002**, *284*, 361–367.

[188] E. R. Weeks and D. A. Weitz, *Phys. Rev. Lett*., **2002**, *89*, 095704–4.

[189] A. Le Grand and G. Petekidis, *Rheol. Acta*, **2007**, *47*, 579–590.

[190] N. Koumakis, A. Pamvouxoglou, A. S. Poulosa and G. Petekidis, *Soft Matter*, **2012**, *8*, 4271–4284.

[191] K. van der Vaart, Y. Rahmani, R. Zargar, D. Bonn and P. Schall, *J. Rheol*., **2013**, *57*, 1195–1209.

[192] L. A. Lyon and A. Fernandez-Nieves, *Annu. Rev. Phys. Chem*., **2012**, *63*, 25–43.

[193] D. M. Heyes, S. M. Clarke and A. C. Brańka, *J. Chem. Phys.,* **2009**, *131*, 204506−11.

[194] D. Vlassopoulos and M. Cloitre, *Curr. Opin. Colloid Interface Sci*., **2014**, *19*, 561–574.

[195] W. C. K. Poon, E. R. Weeks and C. P. Royall, *Soft Matter*, **2012**, *8*, 21–30.

[196] B. Sierra-Martin and A. Fernandez-Nieves, *Soft Matter*, **2012**, *8*, 4141–4150.

[197] E. G. Cohen and I. M. de Schepper, *J. Stat. Phys*., **1991**, *63*, 241–248.

[198] A. J. Liu and S. R. Nagel, *Nature*, **1998**, *396*, 21.

[199] C. S. O'Hern, L. E. Silbert, J. Liu and R. Nagel, *Phys. Rev. E*, **2003**, *68*, 011306−19.

[200] G. Biroli, *Nature Physics*, **2007**, *3*, 222–223.

[201] J. R. Seth, M. Cloitre and R. T. Bonnecaze, *J. Rheol*., **2006**, *50*, 353–376.

[202] R. T. Bonnecaze and M. Cloitre, *Adv. Polym. Sci*., **2010**, *236*, 117–162.

[203] G. Petekidis, D. Vlassopoulos and P. N. Pusey, *J. Phys.:Condens. Matter*, **2004**, *16*, S3955–S3963.

[204] T. G. Mason, J. Bibette and D. A. Weitz, *J. Colloid Interface Sci*., **1996**, *179*, 439–448.

[205] A. Ikeda, L. Berthier and P. Sollich, *Soft Matter*, **2013**, *9*, 7669–7683.

[206] V. Carrier and G. Petekidis, *J. Rheol*., **2009**, *53*, 245–273.

[207] M. Siebenburger, M. Fuchs, H. Winter and M. Ballauff, *J. Rheol*., **2009**, *53*, 707–726.

[208] T. G. Mason and D. A. Weitz, *Phys. Rev. Lett*., **1995**, *75*, 2770–2772.

[209] M. Cloitre, R. Borrega, F. Monti and L. Leibler, *C. R. Physique,* **2003***, 4*, 221–230.

[210] H. Senff and W. Richtering, *J. Chem. Phys*., **1999**, *111*, 1705–1711.

[211] H. Senff, W. Richtering, Ch. Norhausen, A. Weiss and M. Ballauff, *Langmuir*, **1999**, *15*, 102–106.

[212] D. van den Ende, E. H. Purnomo, M. H. G. Duits, W. Richtering and F. Mugele, *Phys. Rev. E*, **2010**, *81*, 011404–9.

[213] W. van Megen and S. M. Underwood, *Phys. Rev. E*, **1994**, *49*, 4206–4220.

[214] H. Gang, A. H. Krall, H. Z. Cummins and D. A. Weitz, *Phys. Rev. E*, **1999**, *59*, 715–721.

[215] J. Mattsson, H. M. Wyss, A. Fernandez-Nieves, K. Miyazaki, Z. Hu, D. R. Reichman and D. A. Weitz, *Nature,* **2009***, 462*, 83–86.

[216] G. Brambilla, D. El Masri, M. Pierno, L. Berthier, L. Cipelletti, G. Petekidis, and A. B. Schofield, *Phys. Rev. Lett*., **2009**, *102*, 085703–4.

[217] E. R. Weeks, J. C. Crocker, A. C. Levitt, A. Schofield and D. A. Weitz, *Science*, **2000**, 287, 627–631.

[218] A. N. St. John, V. Breedveld and L. A. Lyon, *J. Phys. Chem. B*, **2007**, *111*, 7796–7801.

[219] D. Paloli, P. S. Mohanty, J. J. Crassous, E. Zaccarelli and P. Schurtenberger, *Soft Matter*, **2013**, *9*, 3000–3004.

[220] S. E. Paulin, B. J. Ackerson and M. S. Wolfe, *J. Colloid Interface Sci*., **1996**, *178*, 251–262.

[221] J. J. Crassous, M. Siebenbürger, M. Ballauff, M. Drechsler, O. Henrich and M. Fuchs, *J. Chem. Phys*., **2006**, *125*, 204906–11.

[222] U. Gasser, J. S. Hyatt, J.-J. Lietor-Santos, E. S. Herman, L. A. and A. Fernandez-Nieves, *J. Chem. Phys.*, **2014**, *141*, 034901–9.

[223] X. Di, X. Peng and G. B. McKenna, *J. Chem. Phys.*, **2014**, *140*, 054903–9.

[224] E. H. Purnomo, D. van den Ende, S. A. Vanapalli and F. Mugele, *Phys. Rev. Lett.*, **2008**, *101*, 238301–4.

[225] D. Truzzolillo, D. Vlassopoulos and M. Gauthier, *Macromolecules*, **2011**, *44*, 5043–5052.

[226] E. Zaccarelli, C. Mayer, A. Asteriadi, C. N. Likos, F. Sciortino, J. Roovers, H. Iatrou, N. Hadjichristidis, P. Tartaglia, H. Löwen and D. Vlassopoulos,. *Phys. Rev. Lett*., **2005**, *95*, 268301–4.

[227] C. Mayer, E. Zaccarelli, E. Stiakakis, C. N. Likos, F. Sciortino, A. Munam, M. Gauthier, N. Hadjichristidis, H. Iatrou, P. Tartaglia, H. Löwen and D. Vlassopoulos, *Nature Materials*, **2008**, *7*, 780–784.

[228] R. G. Larson in *The Structure and Rheology of Complex Fluids*, Oxford University Press, 1998.

[229] S. Datta in *Tutorial: Rheology of Soft Materials*, Harvard University.

[230] T. G. Mason, Martin-D. Lacasse, G. S. Grest, D. Levine, J. Bibette and D. A. Weitz, *Phys. Rev. E,* **1997**, *56*, 3150–3166.

[231] H. Senff and W. Richtering, *Colloid Polym. Sci*., **2000**, *278*, 830–840.

[232] N. Koumakis, A. B. Schofield and G. Petekidis, *Soft Matter*, **2008**, *4*, 2008–2018.

[233] Z. Zhou, J. V. Hollingsworth, S. Hong, G. Wei, Y Shi, X. Lu, H. Cheng and C. C. Han, *Soft Matter*, **2014**, *10*, 6286–6293.

[234] M. Stieger, J. S. Pedersen, P. Lindner and W. Richtering, *Langmuir*, **2004**, *20*, 7283–7292.

7. Publications and Conference Contributions

7.1 Peer-reviewed Publications

1) *Macro- and Microrheology of Heterogeneous Microgel Packings.*
F. Di Lorenzo and S. Seiffert*, Macromolecules,* **2013**, *46*, 1962–1972.

2) *Particulate and continuum mechanics of microgel pastes: effect and non-effect of compositional heterogeneity.*
F. Di Lorenzo and S. Seiffert, *Colloid Polym. Sci*., **2013**, *291*, 2927–2933.

3) *Tracer Diffusion in Heterogeneous Polymer Networks*.
F. Di Lorenzo and S. Seiffert, *Macromol. Chem. Phys.,* **2014**, *215*, 2097–2111.

4) *Nanostructural heterogeneity in polymer networks and gels.*
F. Di Lorenzo and S. Seiffert, *Polym. Chem.,* **2015**, *6*, 5515–5528.

5) *Counter-effect of Brownian and elastic forces on the liquid-to-solid transition of microgel suspensions.*
F. Di Lorenzo and S. Seiffert, *Soft Matter,* **2015***, 11,* 5235–5245.

6) *Macroscopic and microscopic elasticity of heterogeneous polymer gels*.
F. Di Lorenzo,* J. Hellwig,* R. von Klitzing and S. Seiffert, *ACS Macro Lett.* **2015***, 4,* 698–703.
* Authors contributed equally.

7.2 Publications without Peer-Review Process

7) *Macro- and Micro-Rheology of Heterogeneous Microgel Packings.*
F. Di Lorenzo and S. Seiffert, *Macromol. Chem. Phys.,* **2013***, 214,* F70.

8) *Nanostrukturelle Inhomogenität in Polymernetzwerken.*
F. Di Lorenzo and S. Seiffert, *Nachr. Chem.,* **2014***, 62,* 858–861.

7.3 Conference Contributions

7.3.1 Oral Contributions

1) *"Transports of Actives in Heterogeneous Polymer Networks for Toxin Dialysis"*
F. Di Lorenzo and S. Seiffert, *Helmholtz Virtual Institute Method Workshop 2013*, Teltow, Germany.

2) *"Mechanics and Dynamics of Heterogeneous Polymer Networks"*
F. Di Lorenzo and S. Seiffert, *European Polymer Conference,* EPF 2013, Pisa, Italy.

3) *"Tracer Diffusion in Heterogeneous Polymer Networks"*
F. Di Lorenzo and S. Seiffert, *Berliner Chemie Symposium*, BCS 2014, Berlin, Germany.

4) *"Tracer Diffusion in Heterogeneous Polymer Networks"*
F. Di Lorenzo and S. Seiffert, *IUPAC World Polymer Congress*, MACRO 2014, Chiang Mai, Thailand.

5) *"Shear Elasticity of Colloidal and Granular Microgels: Influence of Particle Size and Softness"*
F. Di Lorenzo and S. Seiffert, *10th Annual European Rheology Conference,* AERC 2105, Nantes, France.

7.3.2 Poster Presentations

6) *"Macro- and Microrheology of Heterogeneous Microgel Packings"*
F. Di Lorenzo and S. Seiffert, *19th Ostwald Kolloquium*, Berlin, Germany.

7) "*Macro- and Microrheology of Heterogeneous Microgel Packings"*
F. Di Lorenzo and S. Seiffert*, Smart Polymers*, Mainz, Germany.

8) "*Macro- and Microrheology of Heterogeneous Microgel Packings"*
F. Di Lorenzo and S. Seiffert, *Makromolekulares Kolloquium 2013*, Freiburg, Germany.

Curriculum Vitae

For reasons of data protection, the curriculum vitae is not included in the online version.

Curriculum Vitae

For reasons of data protection, the curriculum vitae is not included in the online version.